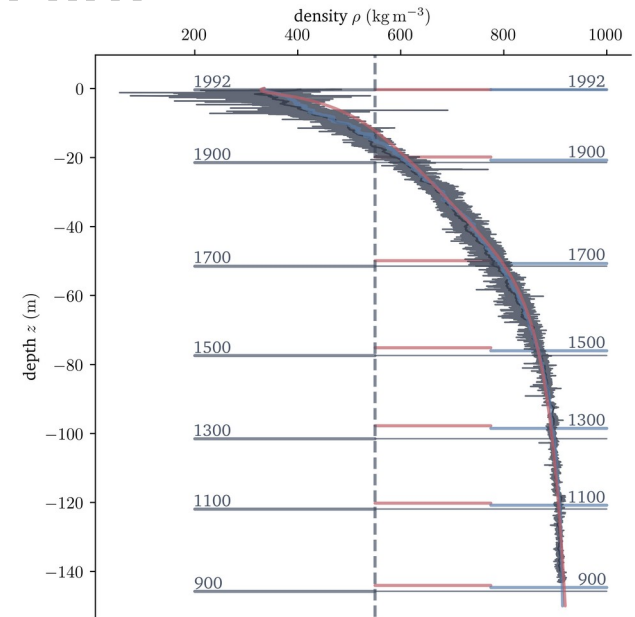
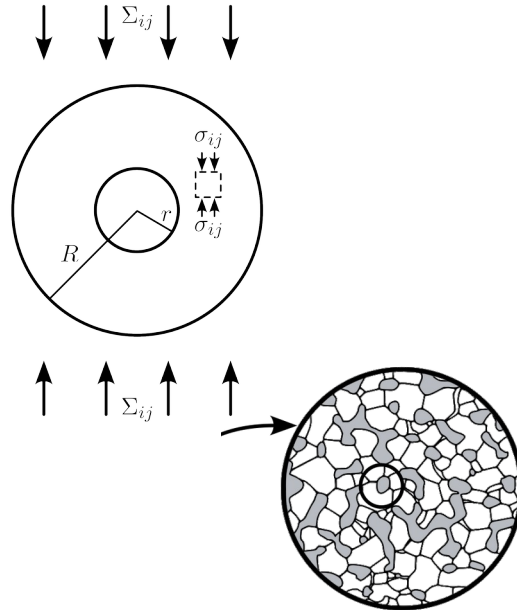
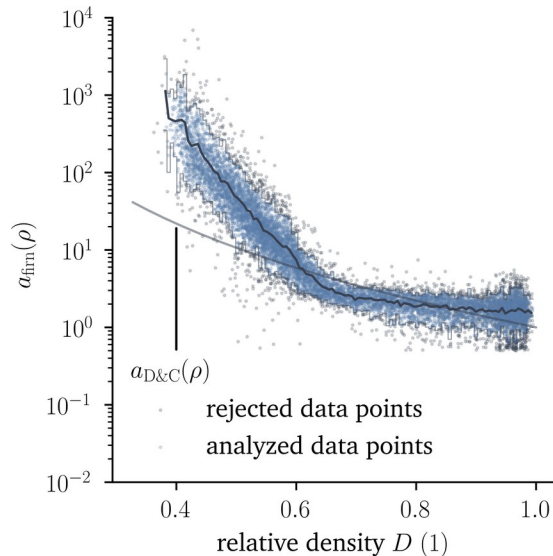
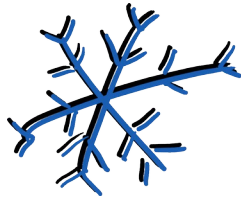


A continuum mechanics perspective on the rheology of firn in the context of firn densification



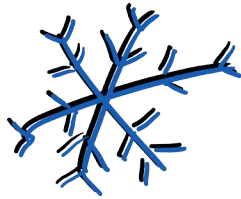
What is firn?

What is firn?



ice

What is firn?



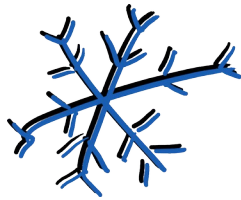
ice

+



air

What is firn?



ice

+



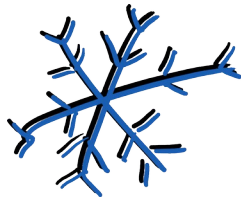
air

=



firn

How can we describe the rheology of firn?



ice

+



air

=



firn

How can we describe the rheology of firn?



How can we describe the rheology of firn?



How can we describe the rheology of firn?



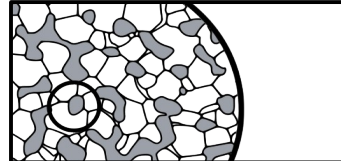
How can we describe the rheology of firn?



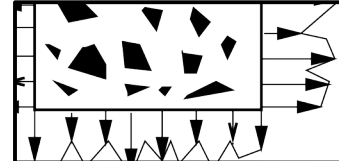
mixture of
ice, air, (liquid water)



The Material



Micro-Macro



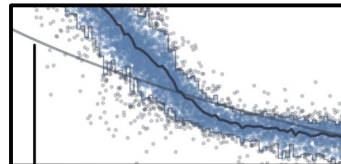
Cell-Model

$$S = (a(\rho) \Sigma_e^2 +$$

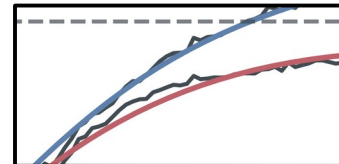
Effective Stress

$$\zeta(\rho, T, \dot{E}_{ij})$$

Material Model



Model Inversion



Material Behavior



Examples



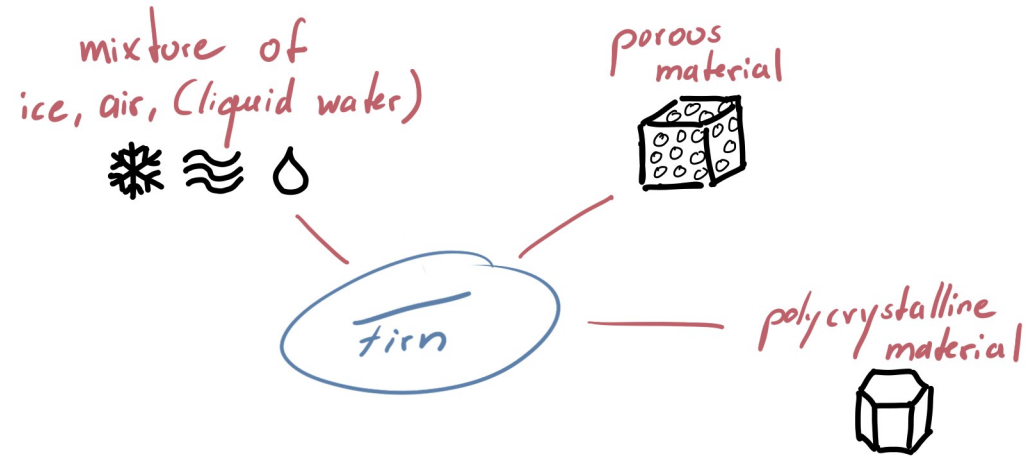


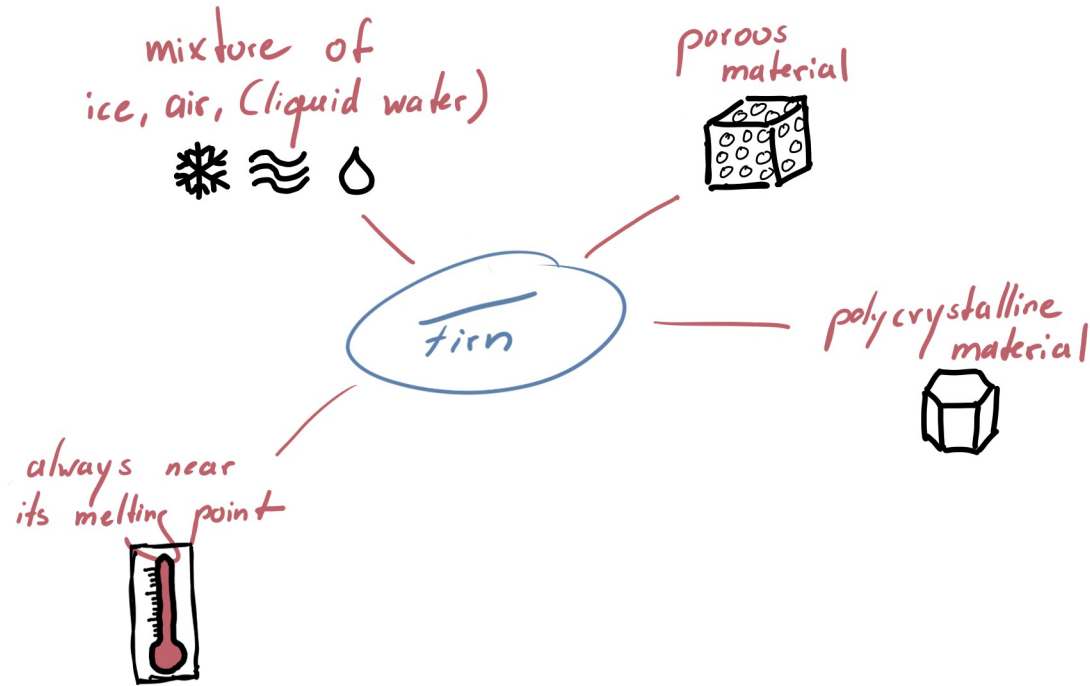
mixture of
ice, air, (liquid water)

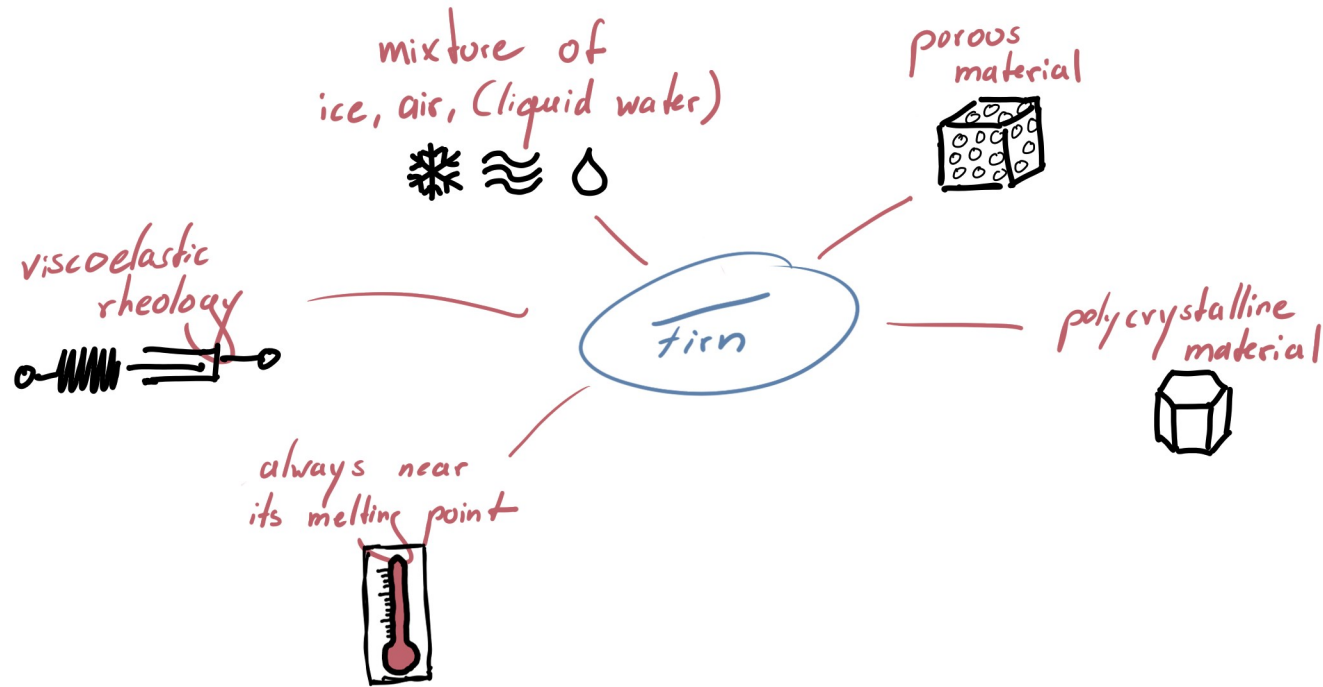


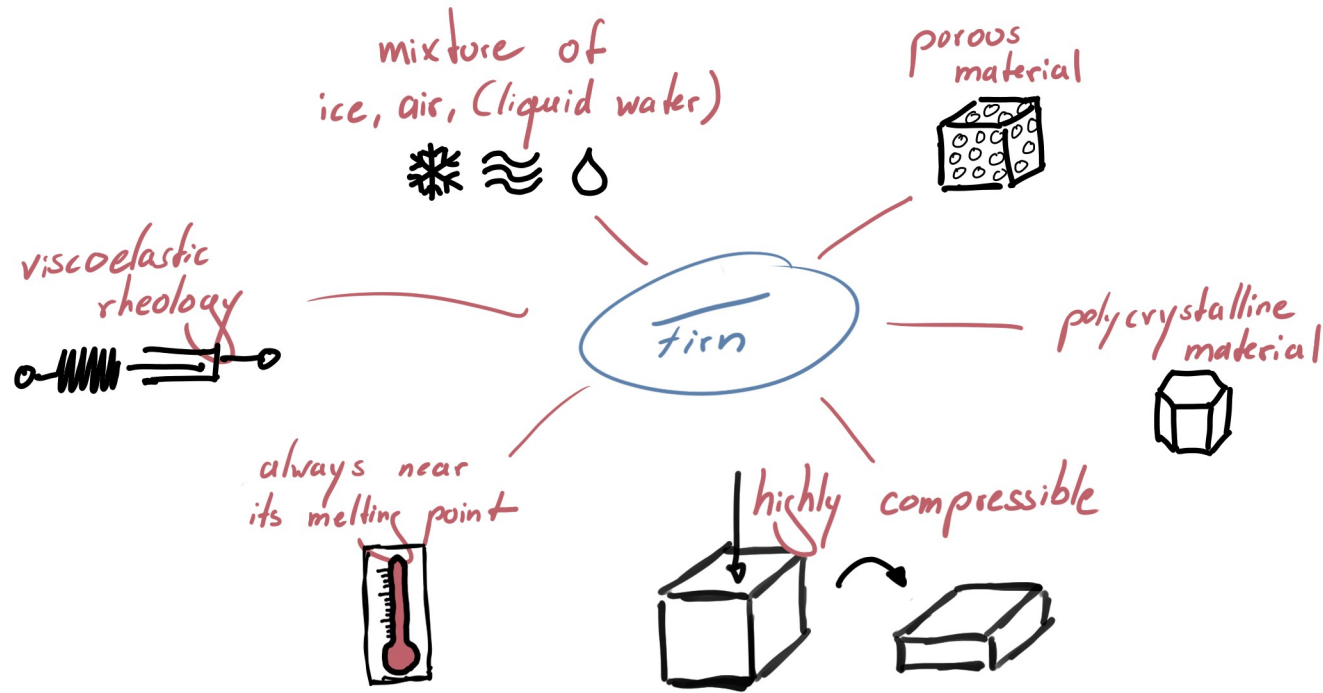
polycrystalline
material



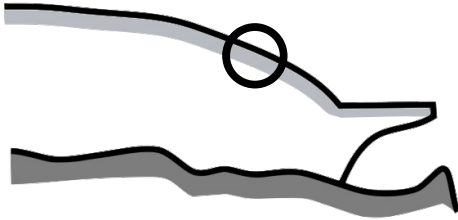




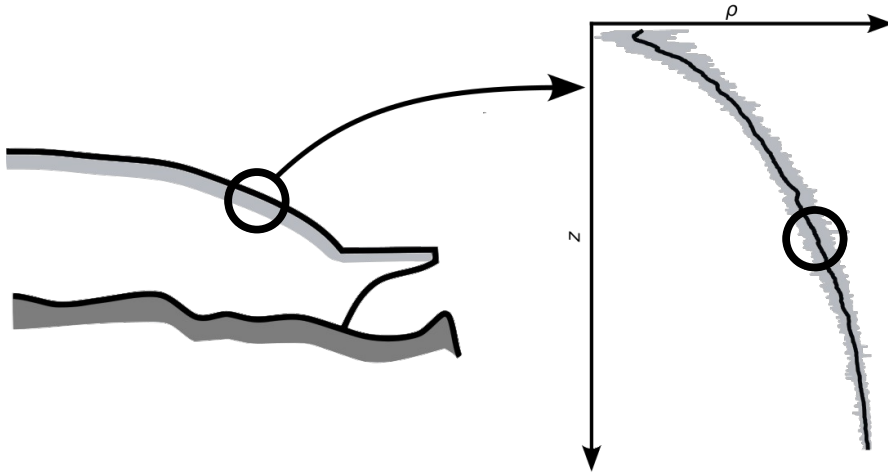




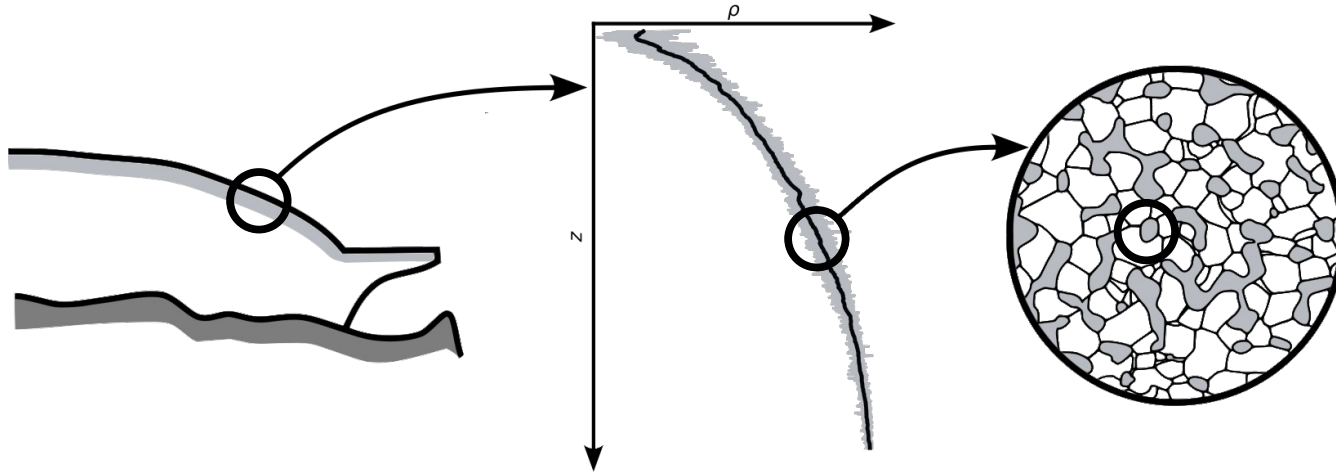
From the macro-scale to the micro-scale



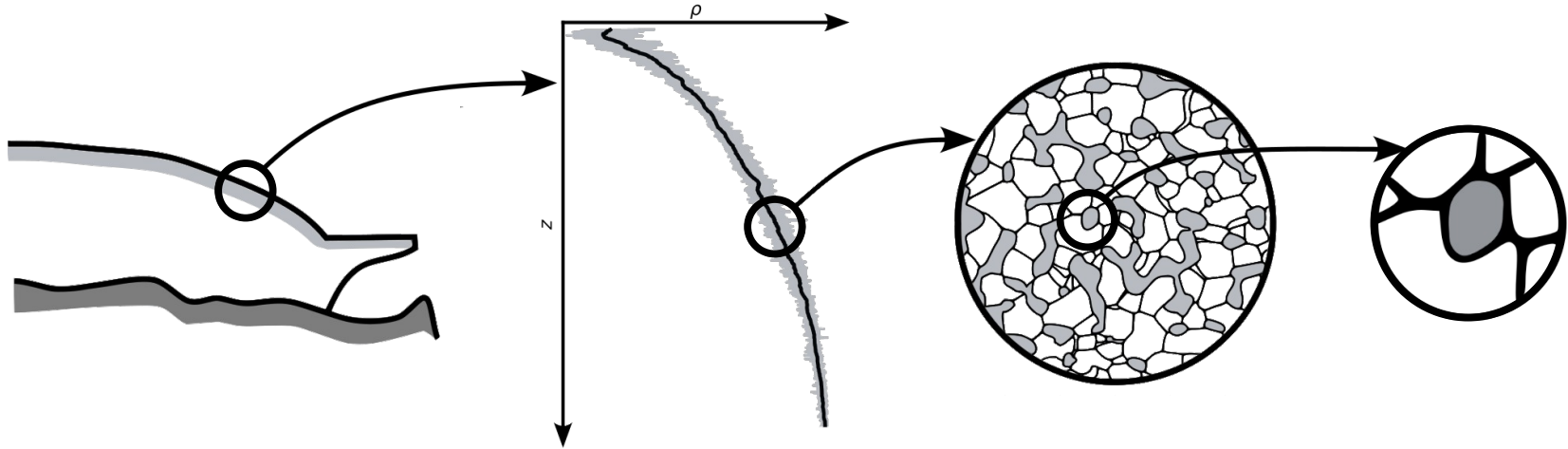
From the macro-scale to the micro-scale



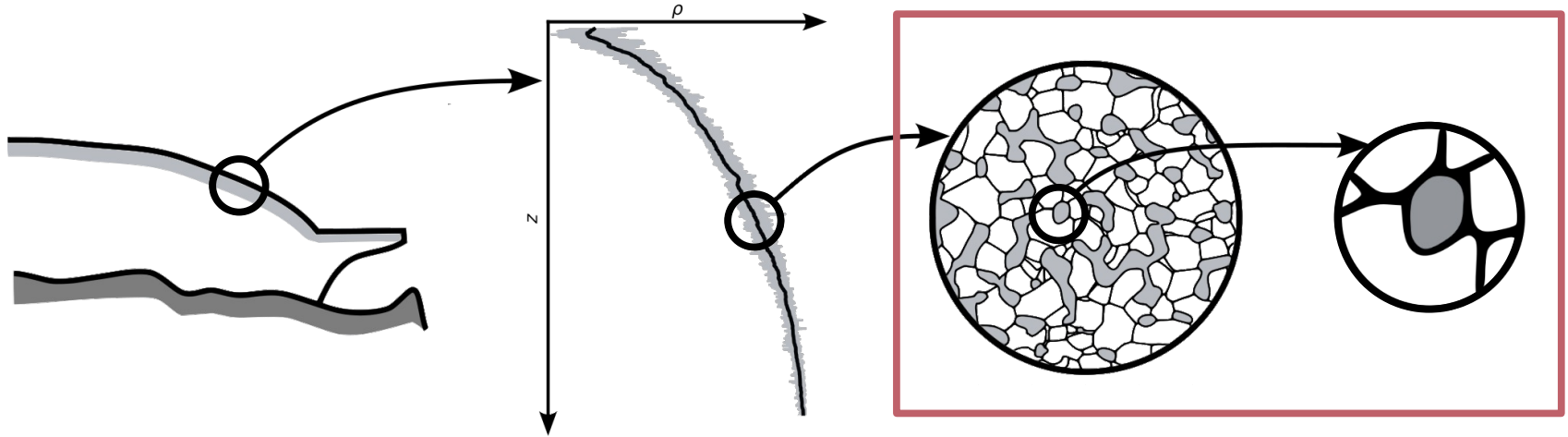
From the macro-scale to the micro-scale



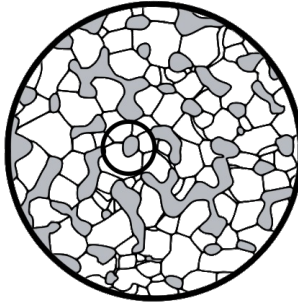
From the macro-scale to the micro-scale



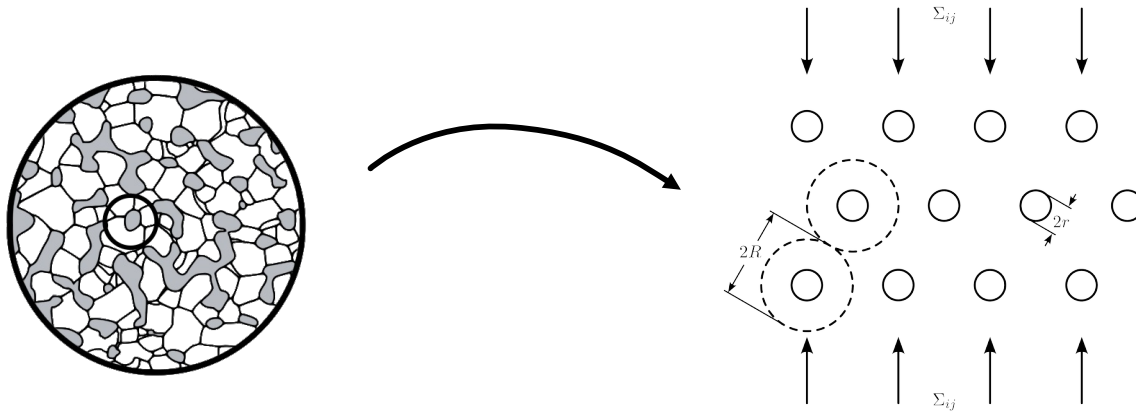
From the macro-scale to the micro-scale



From the macro-scale to the micro-scale

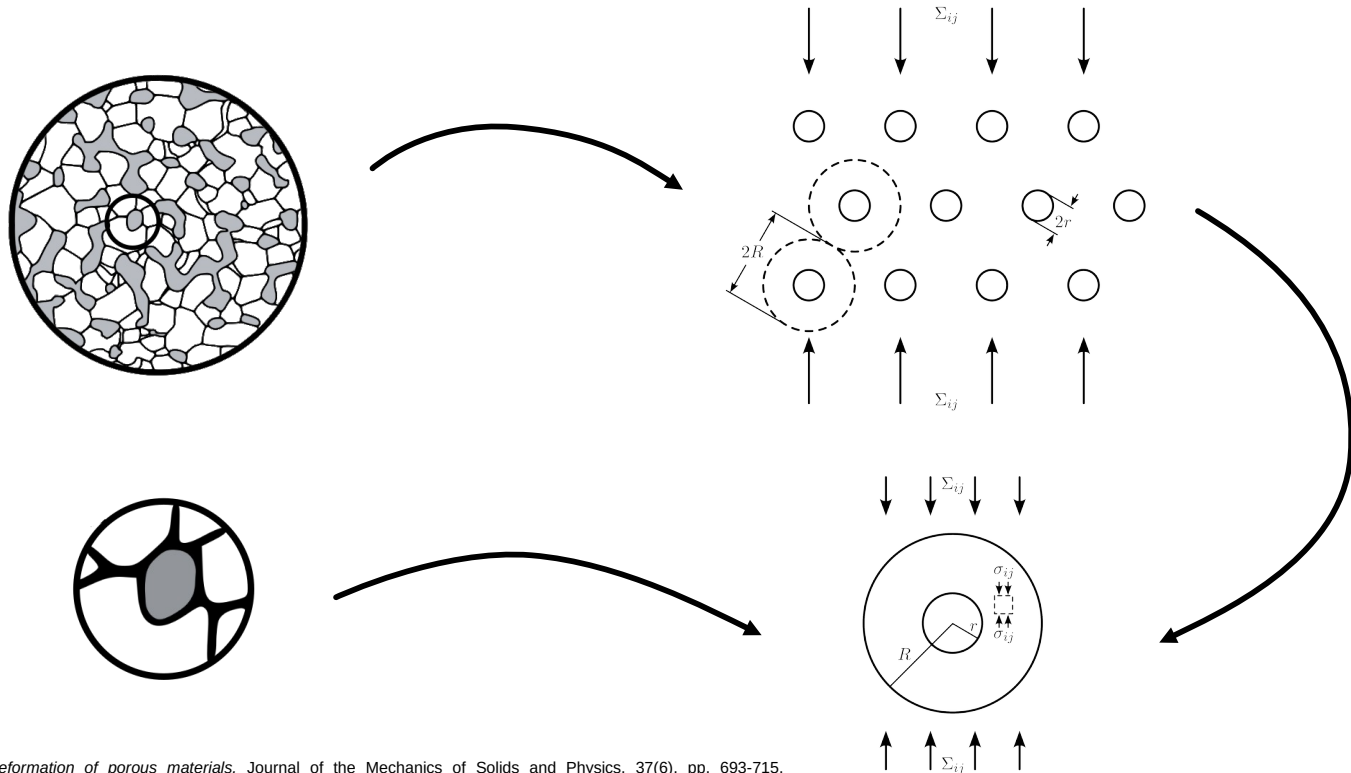


From the macro-scale to the micro-scale

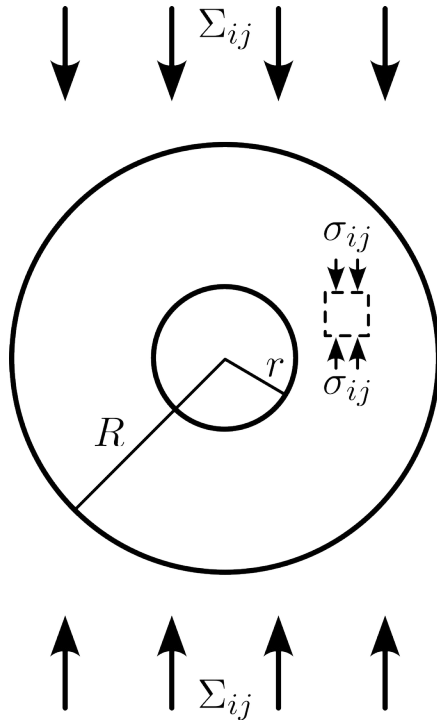


Cocks, A. C. F. (1989). *Inelastic deformation of porous materials*. Journal of the Mechanics of Solids and Physics, 37(6), pp. 693-715.
[https://doi.org/https://doi.org/10.1016/0022-5096\(89\)90014-8](https://doi.org/https://doi.org/10.1016/0022-5096(89)90014-8)

From the macro-scale to the micro-scale



Cocks, A. C. F. (1989). *Inelastic deformation of porous materials*. Journal of the Mechanics of Solids and Physics, 37(6), pp. 693-715.
[https://doi.org/https://doi.org/10.1016/0022-5096\(89\)90014-8](https://doi.org/https://doi.org/10.1016/0022-5096(89)90014-8)



macro-scale

$$\Sigma_{ij}$$

macroscopic
stress tensor

$$\dot{E}_{ij}$$

macroscopic
strain rate tensor

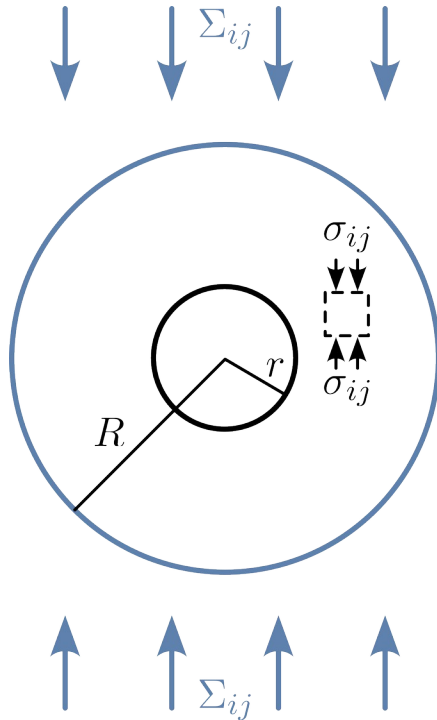
micro-scale

$$\sigma_{ij}$$

microscopic
stress tensor

$$\dot{\epsilon}_{ij}$$

microscopic
strain rate tensor



macro-scale

micro-scale

$$\Sigma_{ij}$$

macroscopic
stress tensor

$$\sigma_{ij}$$

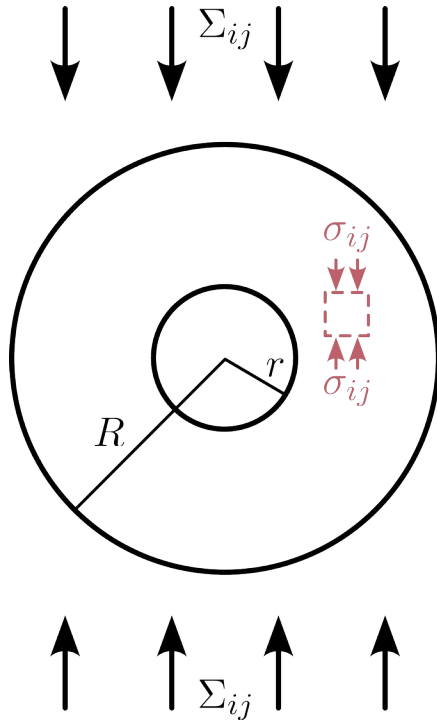
microscopic
stress tensor

$$\dot{E}_{ij}$$

macroscopic
strain rate tensor

$$\dot{\epsilon}_{ij}$$

microscopic
strain rate tensor



macro-scale

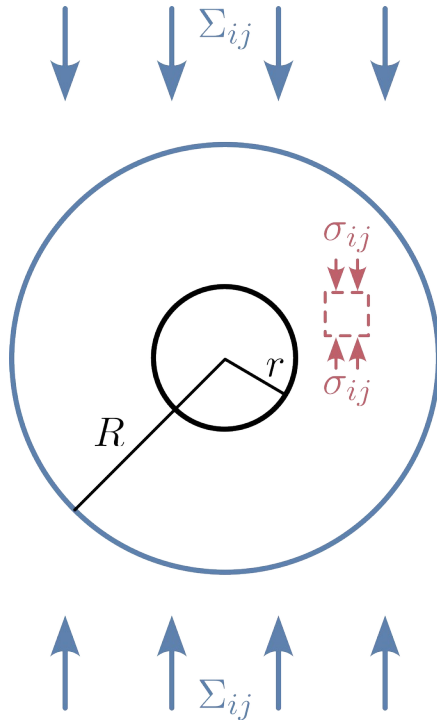
Σ_{ij} macroscopic stress tensor

\dot{E}_{ij} macroscopic strain rate tensor

micro-scale

σ_{ij} microscopic stress tensor

$\dot{\epsilon}_{ij}$ microscopic strain rate tensor



macro-scale

Σ_{ij} macroscopic stress tensor

\dot{E}_{ij} macroscopic strain rate tensor

micro-scale

σ_{ij} microscopic stress tensor

$\dot{\epsilon}_{ij}$ microscopic strain rate tensor

Annals of Glaciology 24 1997
© International Glaciological Society

Flow simulation of a firn-covered cold glacier

OLIVIER GAGLIARDINI, JACQUES MEYSSONNIER
*Laboratoire de Glaciologie et Géophysique de l'Environnement du CNRS,
associé à l'Université Joseph Fourier (UJF-Grenoble I), BP 96, 38402 Saint-Martin-d'Hères Cedex, France*

A full Stokes-flow thermo-mechanical model for firn and ice applied to the Gorshkov crater glacier, Kamchatka

Thomas ZWINGER,¹ Ralf GREVE,² Olivier GAGLIARDINI,³ Takayuki SHIRAIWA,⁴
Mikko LYL¹

¹*CSC–Scientific Computing Ltd., P.O. Box 405, FIN-02101 Espoo, Finland*
E-mail: thomas.zwinger@csc.fi

²*Institute of Low Temperature Science, Hokkaido University, Kita-19, Nishi-8, Kita-ku, Sapporo 060–0819, Japan*

³*LGGE CNRS-UJF Grenoble I, BP 96, 38402 Saint Martin d’Hères, France*

⁴*Research Institute for Humanity and Nature, 457–4, Motoyama, Kamigamo, Kita-ku, Kyoto 603–8047, Japan*

Journal of Glaciology



A full Stokes ice-flow model to assist the interpretation of millennial-scale ice cores at the high-Alpine drilling site Colle Gnifetti, Swiss/Italian Alps

Carlo Licciulli^{1,2} , Pascal Bohleber^{2,3,†}, Josef Lier^{2,3}, Olivier Gagliardini⁴ ,
Martin Hoelzle⁵  and Olaf Eisen^{6,7} 

Licciulli, C., Bohleber, P., Lier, J., Gagliardini, O., Hoelzle, M., and Eisen, O. (2020). A full Stokes ice-flow model to assist the interpretation of millennial-scale ice cores at the high-Alpine drilling site Colle Gnifetti, Swiss/Italian Alps. *Journal of Glaciology*, 66(255), pp. 35-48. <https://doi.org/10.1017/jog.2019.82>

Budiansky, B., Hutchinson, J. W., and Slutsky, S. (1982). *Void Growth and Collapse in Viscous Solids.* Mechanics of Solids, The Rodney Hill 60th Anniversary Volume, pp. 13-45. <https://doi.org/10.1016/B978-0-08-025443-2.50009-4>

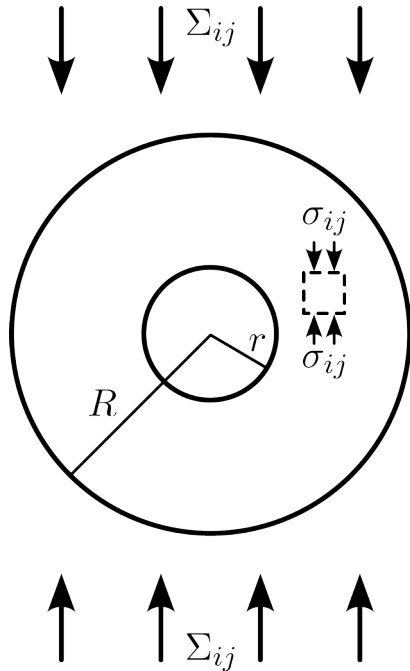
Cocks, A. C. F. (1989). *Inelastic deformation of porous materials.* Journal of the Mechanics and Physics of Solids, 37(6), pp. 693-715. [https://doi.org/10.1016/0022-5096\(89\)90014-8](https://doi.org/10.1016/0022-5096(89)90014-8)

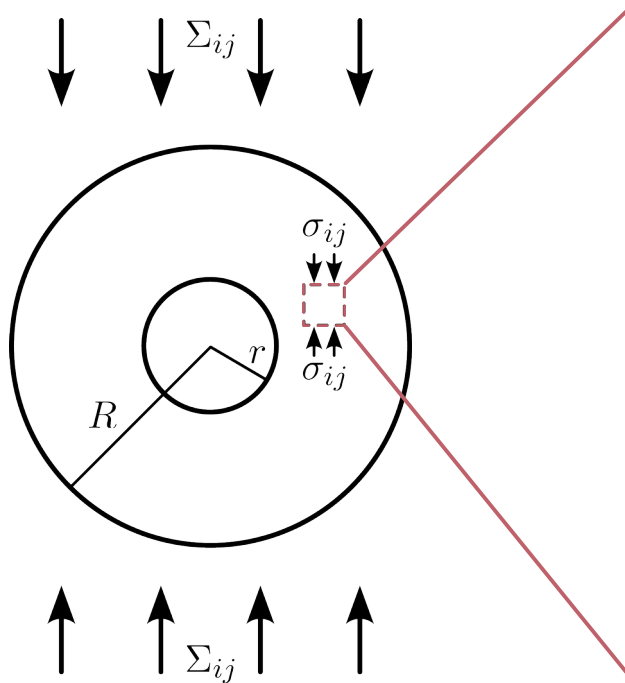
Ponte Castaneda, P. (1991). *The effective mechanical properties of nonlienaar isotropic composites.* Journal of the Mechanics and Physics of Solids, 39(1), pp. 45-71. [https://doi.org/10.1016/0022-5096\(91\)90030-R](https://doi.org/10.1016/0022-5096(91)90030-R)

Sofronis, P. and McMeeking, R. M. (1992). *Creep of Power-Law Material Containing Spherical Voids.* Journal of Applied Mechanics, 59(S2), pp. S88-S95. <https://doi.org/10.1115/1.2899512>

Duva, J. M. and Crow, P. D. (1992). *The densification of powders by power-law creep during hot isostatic pressing.* Acta Metallurgica et Materialia, 40(1), pp. 31-34. [https://doi.org/10.1016/0956-7151\(92\)90196-L](https://doi.org/10.1016/0956-7151(92)90196-L)

Duva, J. M. and Crow, P. D. (1994). *Analysis of consolidation of reinforced materials by power-law creep.* Mechanics of Materials, 17(1), pp. 25-32. [https://doi.org/10.1016/0167-6636\(94\)90011-6](https://doi.org/10.1016/0167-6636(94)90011-6)





Glen's Flow Law (Glen, 1955)

$\dot{\epsilon}_e, \tilde{\Phi}$

$$\dot{\epsilon}_e = B\sigma_e^n$$

(Nye's) generalization of Glen's Flow Law (Nye, 1957)

$$\dot{\epsilon}_{ij} = \frac{3}{2} B\sigma_e^{(n-1)} s_{ij}$$

flow potential

$$\tilde{\Phi} = \frac{1}{(n+1)} B^* \sigma_e^{(n+1)}$$

Glen, J. W. (1955). *The creep of polycrystalline ice*. Proceedings of the Royal Society A, 228(1175), pp. 519-538.

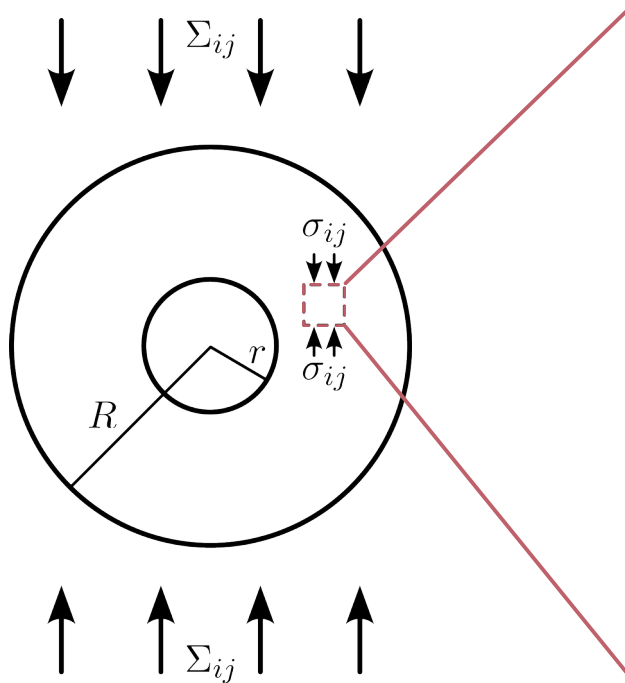
<https://doi.org/10.1098/rspa.1955.0066>

Nye, J. F. (1957). *The distribution of stress and velocity in glaciers and ice-sheets*. Proceedings of the Royal Society A, 238(1216), pp. 113-133.

<https://doi.org/10.1098/rspa.1957.0026>

Cocks, A. C. F. (1989). *Inelastic deformation of porous materials*. Journal of the Mechanics of Solids and Physics, 37(6), pp. 693-715.

[https://doi.org/10.1016/0022-5096\(89\)90014-8](https://doi.org/10.1016/0022-5096(89)90014-8)



Glen's Flow Law (Glen, 1955)

$$\sigma_e = B^{-\frac{1}{n}} \dot{\epsilon}_e^{\frac{1}{n}}$$

σ_e, Φ

(Nye's) generalization of Glen's Flow Law (Nye, 1957)

$$\dot{\epsilon}_{ij} = \frac{3}{2} B^{\frac{1}{n}} \dot{\epsilon}_e^{\frac{(n-1)}{n}} s_{ij}$$

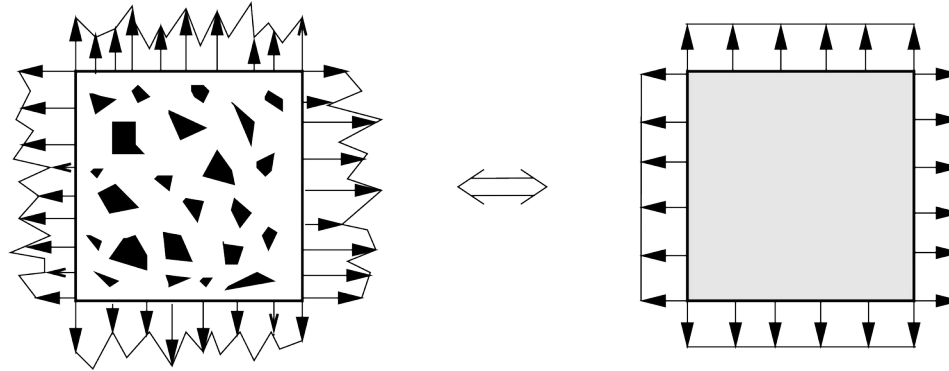
strain energy rate density

$$\Phi = \frac{n}{(n+1)} B^* - \frac{1}{n} \dot{\epsilon}_e^{\frac{(n+1)}{n}}$$

Glen, J. W. (1955). *The creep of polycrystalline ice*. Proceedings of the Royal Society A, 228(1175), pp. 519-538.
<https://doi.org/10.1098/rspa.1955.0066>

Nye, J. F. (1957). *The distribution of stress and velocity in glaciers and ice-sheets*. Proceedings of the Royal Society A, 238(1216), pp. 113-133.
<https://doi.org/10.1098/rspa.1957.0026>

Cocks, A. C. F. (1989). *Inelastic deformation of porous materials*. Journal of the Mechanics of Solids and Physics, 37(6), pp. 693-715.
[https://doi.org/10.1016/0022-5096\(89\)90014-8](https://doi.org/10.1016/0022-5096(89)90014-8)



Representative volume element with fluctuating microscopic fields and averages illustrating the Hill Condition (Gross and Seelig, 2018, p. 266).

$$\Sigma_{ij} \dot{E}_{ij} = \frac{1}{V} \int_V \sigma_{ij} \dot{\epsilon}_{ij} dV$$

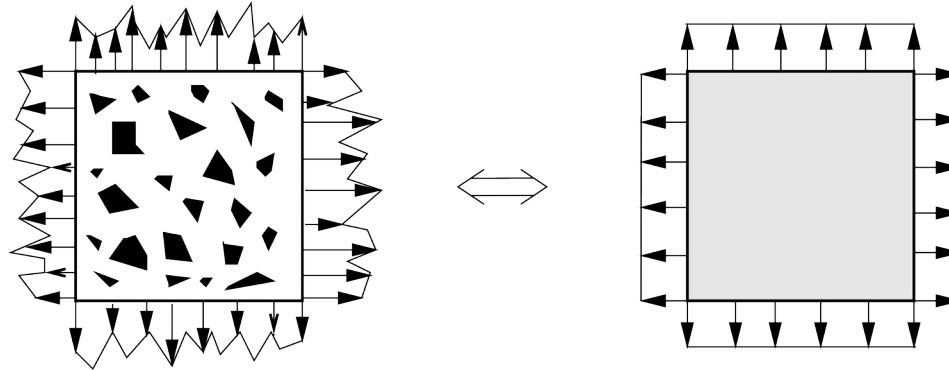
(Hill, 1963)

Hill, R. (1963). *Elastic properties of reinforced solids: Some theoretical principles*. Journal of Mechanics and Physics of Solids, 11(5), pp. 357-372.

[https://doi.org/10.1016/0022-5096\(63\)90036-Xfs](https://doi.org/10.1016/0022-5096(63)90036-Xfs)

Gross, D. and Seelig, T. (2018). *Fracture Mechanics With an Introduction to Micromechanics*. Ed. by Kulack, F. A., 3rd ed. Mechanical Engineering Series. Springer. <https://doi.org/10.1007/978-3-319-71090-7>

Macro-Scale Flow Potential



Representative volume element with fluctuating microscopic fields and averages illustrating the Hill Condition (Gross and Seelig, 2018, p. 266).

$$\Sigma_{ij} \dot{E}_{ij} = \frac{1}{V} \int_V \sigma_{ij} \dot{\epsilon}_{ij} dV$$

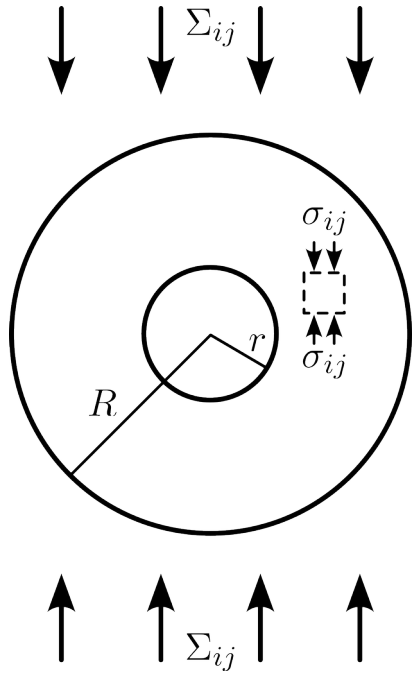
(Hill, 1963)

Hill, R. (1963). *Elastic properties of reinforced solids: Some theoretical principles*. Journal of Mechanics and Physics of Solids, 11(5), pp. 357-372.

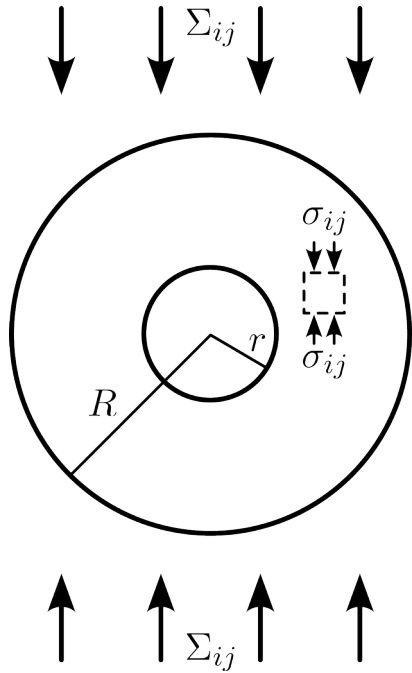
[https://doi.org/10.1016/0022-5096\(63\)90036-Xfs](https://doi.org/10.1016/0022-5096(63)90036-Xfs)

Gross, D. and Seelig, T. (2018). *Fracture Mechanics With an Introduction to Micromechanics*. Ed. by Kulack, F. A., 3rd ed. Mechanical Engineering Series. Springer. <https://doi.org/10.1007/978-3-319-71090-7>

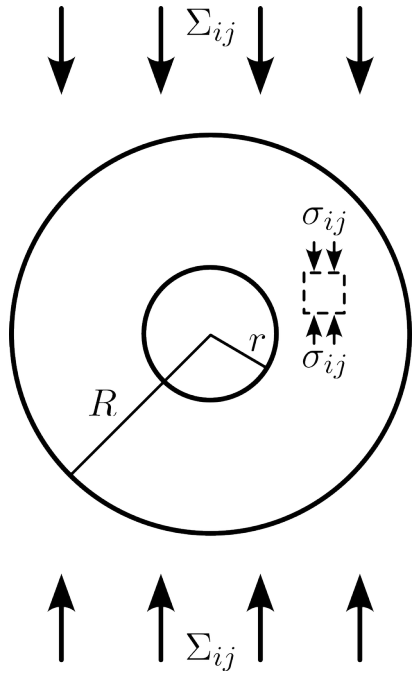
Macro-Scale Flow Potential



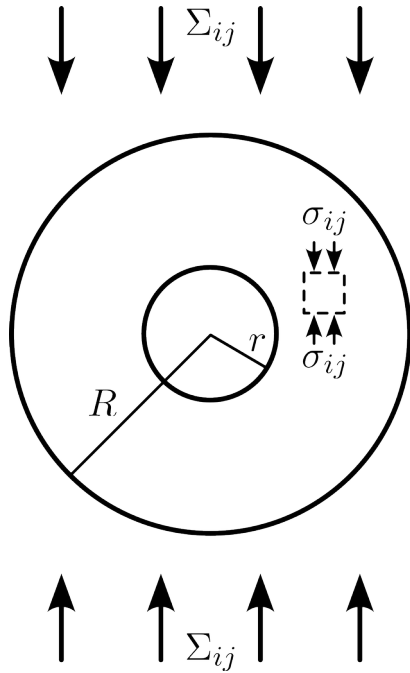
$$\Sigma_{ij} \dot{E}_{ij} = \frac{1}{V} \int_V \sigma_{ij} \dot{\epsilon}_{ij} dV$$



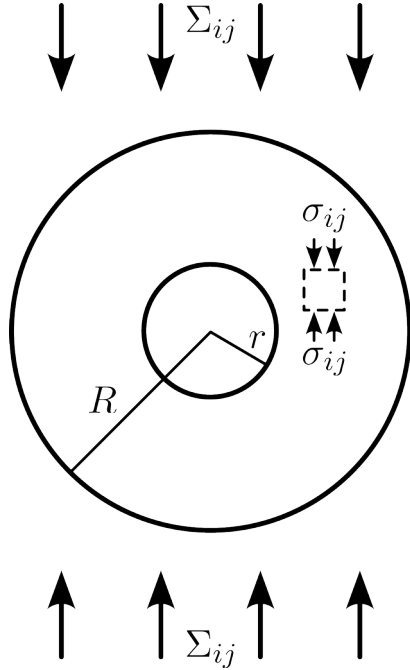
$$\Sigma_{ij} \dot{E}_{ij} = \frac{1}{V} \int_{V_m} \sigma_{ij} \dot{\epsilon}_{ij} dV$$



$$d\tilde{\Psi} = d\Sigma_{ij}\dot{E}_{ij} = \frac{1}{V} \int_{V_m} d\sigma_{ij}\dot{\epsilon}_{ij} dV$$



$$d\Psi = \frac{1}{V} \int_{V_m} d\tilde{\Phi} dV$$



$$\tilde{\Psi} = \frac{1}{V} \int_{V_m} \tilde{\Phi} dV$$

$$\tilde{\Phi} = \frac{1}{(n+1)} B^* \sigma_e^{(n+1)}$$

micro-scale
flow potential

$$\tilde{\Psi} = \frac{1}{(n+1)} B^* S^{(n+1)}$$

macro-scale
flow potential

$$S_{\text{Cocks}}^2 = \frac{\left(1 + \frac{2}{3}(1 - D)\right)}{D^{2n/(n+1)}} \Sigma_e^2 + \frac{\frac{9}{4} \frac{2n}{(n+1)} \frac{(1-D)}{(2-D)}}{D^{2n/(n+1)}} \Sigma_m^2$$

Cocks, A. C. F. (1989). *Inelastic deformation of porous materials*. Journal of the Mechanics of Solids and Physics, 37(6), pp. 693-715. [https://doi.org/10.1016/0022-5096\(89\)90014-8](https://doi.org/10.1016/0022-5096(89)90014-8)

effective stress comparison

$$S_{\text{Cocks}}^2 = \frac{\left(1 + \frac{2}{3}(1 - D)\right)}{D^{2n/(n+1)}} \Sigma_e^2 + \frac{\frac{9}{4} \frac{2n}{(n+1)} \frac{(1-D)}{(2-D)}}{D^{2n/(n+1)}} \Sigma_m^2$$

Cocks, A. C. F. (1989). *Inelastic deformation of porous materials*. Journal of the Mechanics of Solids and Physics, 37(6), pp. 693-715. [https://doi.org/10.1016/0022-5096\(89\)90014-8](https://doi.org/10.1016/0022-5096(89)90014-8)

$$S_{\text{WilkinsonAshby}}^2 = \left(\frac{n(1-D)}{\left(1 - (1-D)^{1/n}\right)^n} \right)^{2/(n+1)} \left(\frac{3}{2n} \right)^2 \Sigma_m^2$$

Wilkinson, D. S. and Ashby, M. F. (1975). *Pressure sintering by power law creep*. Acta Metallurgica, 23(11), pp. 1277-1285. [https://doi.org/10.1016/0001-6160\(75\)90136-4](https://doi.org/10.1016/0001-6160(75)90136-4)

effective stress comparison

$$S_{\text{Cocks}}^2 = \frac{\left(1 + \frac{2}{3}(1 - D)\right)}{D^{2n/(n+1)}} \Sigma_e^2 + \frac{\frac{9}{4} \frac{2n}{(n+1)} \frac{(1-D)}{(2-D)}}{D^{2n/(n+1)}} \Sigma_m^2$$

Cocks, A. C. F. (1989). *Inelastic deformation of porous materials*. Journal of the Mechanics of Solids and Physics, 37(6), pp. 693-715. [https://doi.org/10.1016/0022-5096\(89\)90014-8](https://doi.org/10.1016/0022-5096(89)90014-8)

$$S_{\text{WilkinsonAshby}}^2 = \left(\frac{n(1-D)}{\left(1 - (1-D)^{1/n}\right)^n} \right)^{2/(n+1)} \left(\frac{3}{2n} \right)^2 \Sigma_m^2$$

Wilkinson, D. S. and Ashby, M. F. (1975). *Pressure sintering by power law creep*. Acta Metallurgica, 23(11), pp. 1277-1285. [https://doi.org/10.1016/0001-6160\(75\)90136-4](https://doi.org/10.1016/0001-6160(75)90136-4)

$$S_{\text{D\&C}}^2 = \frac{\left(1 + \frac{2}{3}(1 - D)\right)}{D^{2n/(n+1)}} \Sigma_e^2 + \left(\frac{n(1-D)}{\left(1 - (1-D)^{1/n}\right)^n} \right)^{2/(n+1)} \left(\frac{3}{2n} \right)^2 \Sigma_m^2$$

Duva, J. M. and Crow, P. D. (1994). *Analysis of consolidation of reinforced materials by power-law creep*. Mechanics of Materials, 17(1), pp. 25-32. [https://doi.org/10.1016/0167-6636\(94\)90011-6](https://doi.org/10.1016/0167-6636(94)90011-6)

effective stress comparison

$$S_{D\&C}^2 = \frac{\left(1 + \frac{2}{3}(1 - D)\right)}{D^{2n/(n+1)}} \Sigma_e^2 + \left(\frac{n(1 - D)}{\left(1 - (1 - D)^{1/n}\right)^n}\right)^{2/(n+1)} \left(\frac{3}{2n}\right)^2 \Sigma_m^2$$

Duva, J. M. and Crow, P. D. (1994). *Analysis of consolidation of reinforced materials by power-law creep*. *Mechanics of Materials*, 17(1), pp. 25-32. [https://doi.org/10.1016/0167-6636\(94\)90011-6](https://doi.org/10.1016/0167-6636(94)90011-6)

general form of the effective stress

$$S = \left(a(\rho) \Sigma_e^2 + b(\rho) \Sigma_m^2\right)^{\frac{1}{2}}$$

with von Mises equivalent stress

$$\Sigma_e^2 = \frac{3}{2} \Sigma_{ij}^D \Sigma_{ij}^D$$

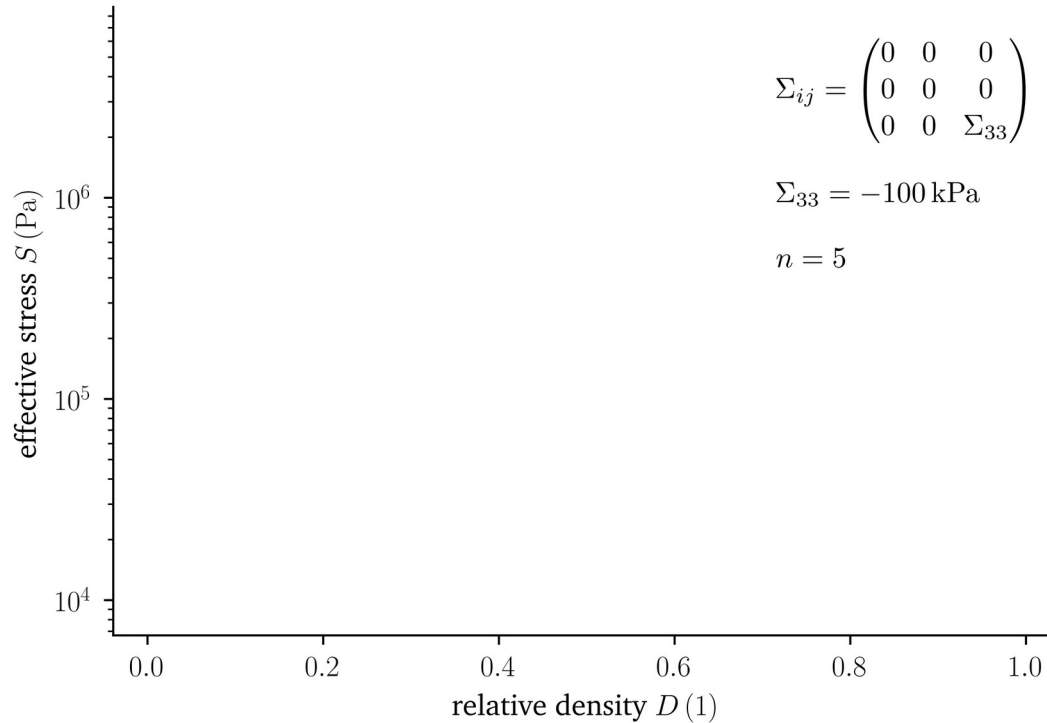
deviatoric stress tensor

$$\Sigma_{ij}^D = \Sigma_{ij} - \frac{1}{3} \Sigma_{kk} \delta_{ij}$$

mean stress

$$\Sigma_m = \frac{1}{3} \Sigma_{kk}$$

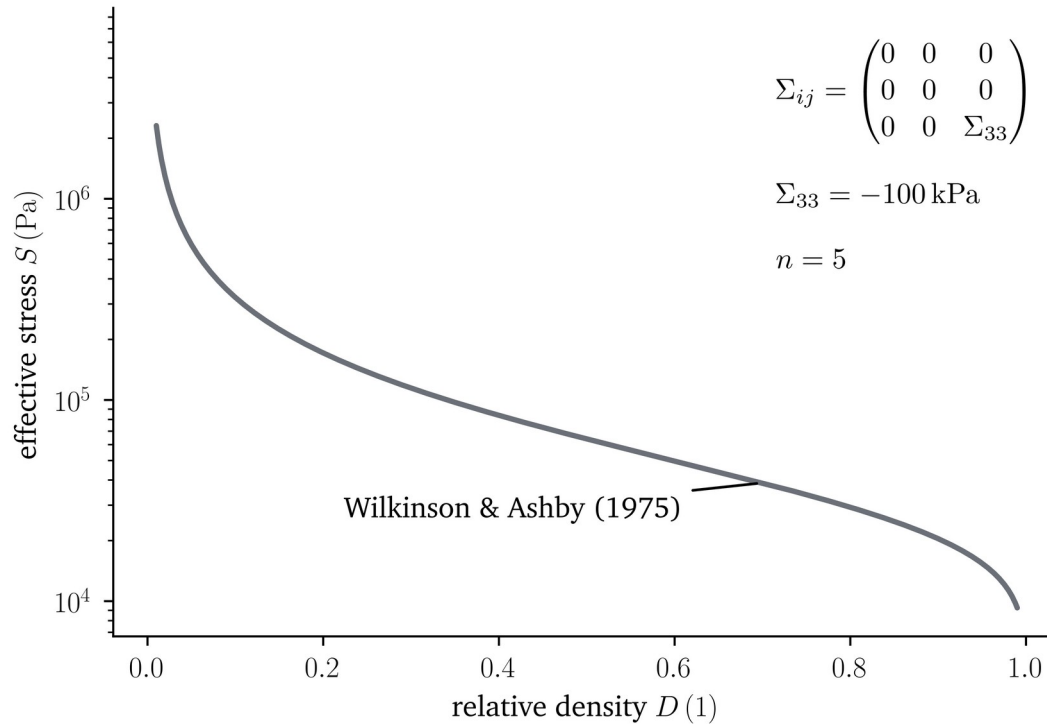
effective stress comparison



Wilkinson and Ashby (1975)

Cocks (1989)

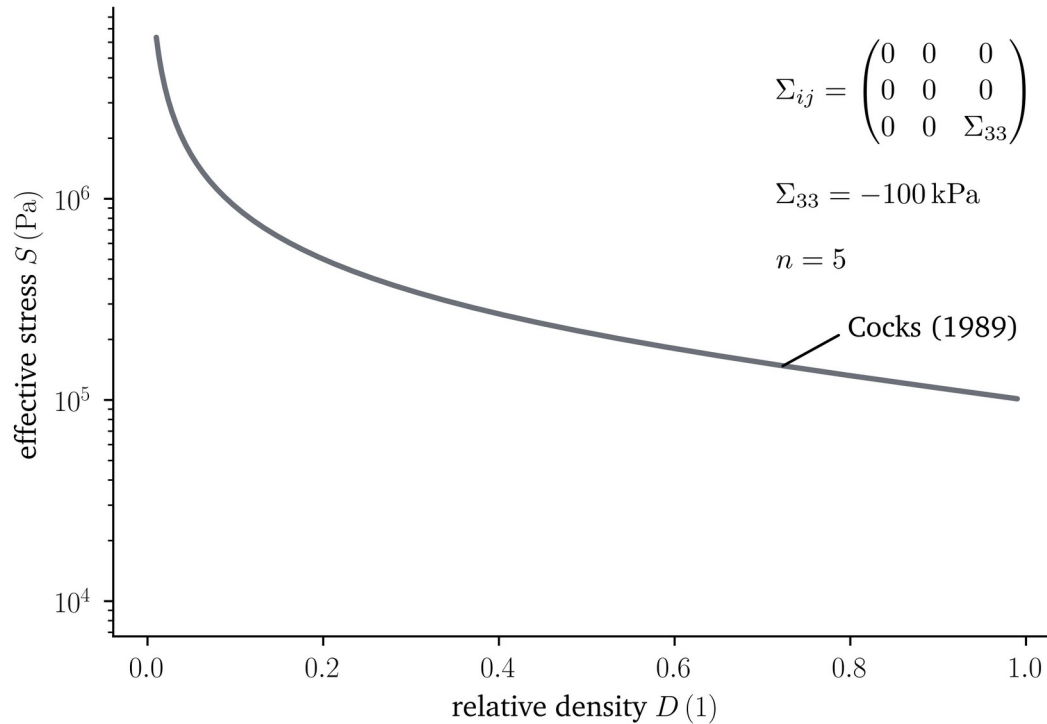
Duva and Crow (1994)



Wilkinson and Ashby (1975)

Cocks (1989)

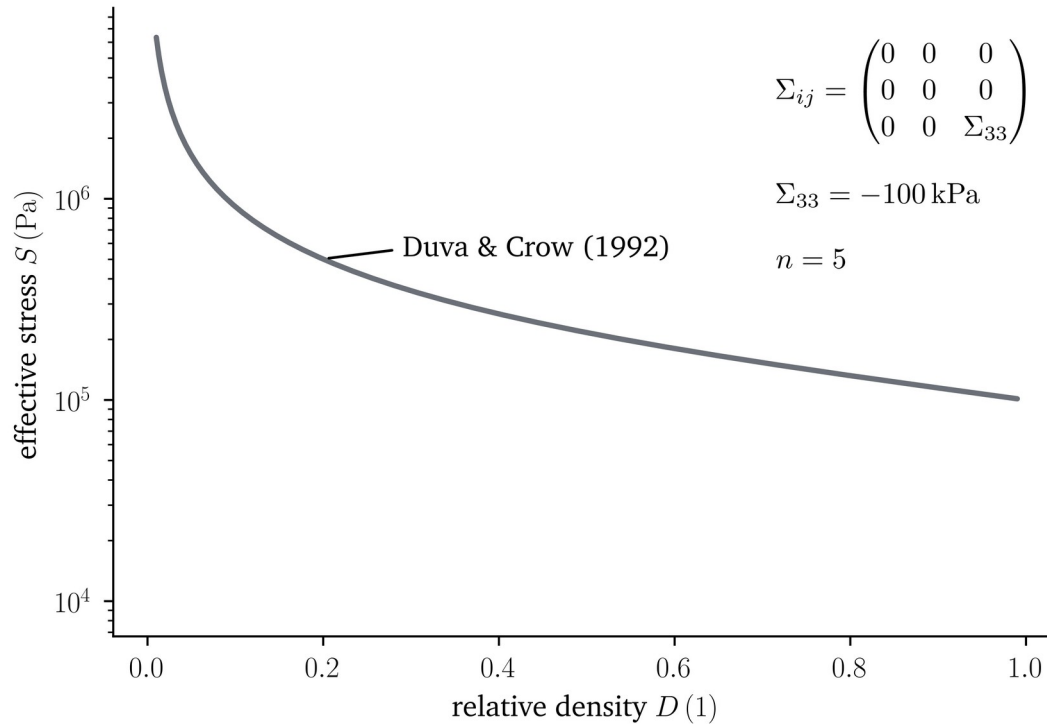
Duva and Crow (1994)



Wilkinson and Ashby (1975)

Cocks (1989)

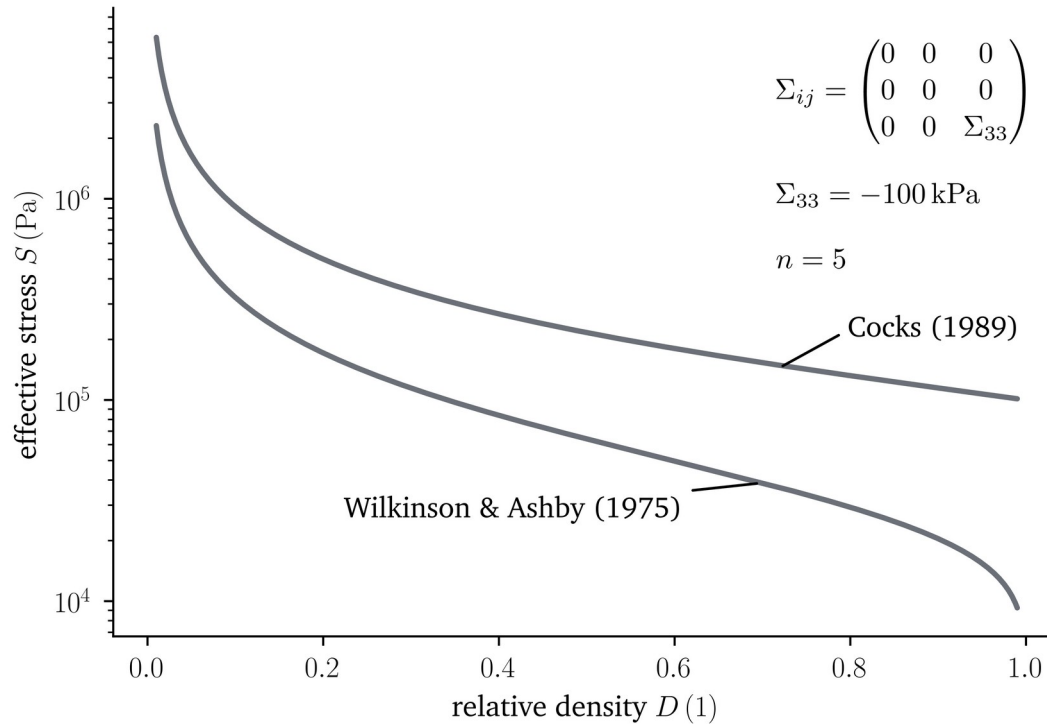
Duva and Crow (1994)



Wilkinson and Ashby (1975)

Cocks (1989)

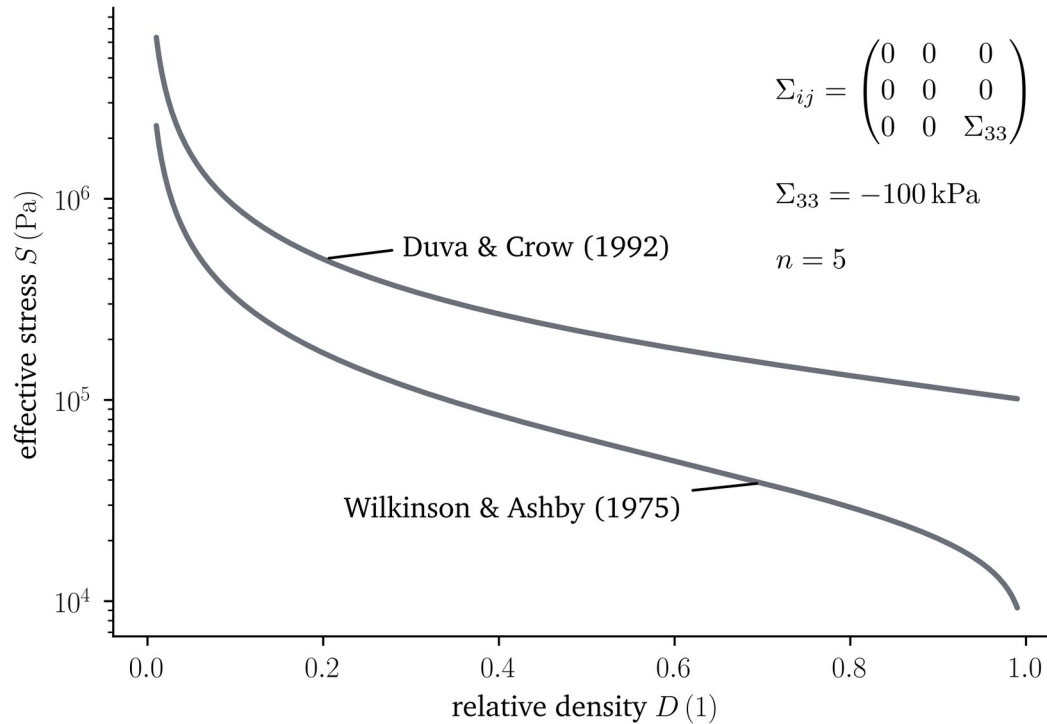
Duva and Crow (1994)



Wilkinson and Ashby (1975)

Cocks (1989)

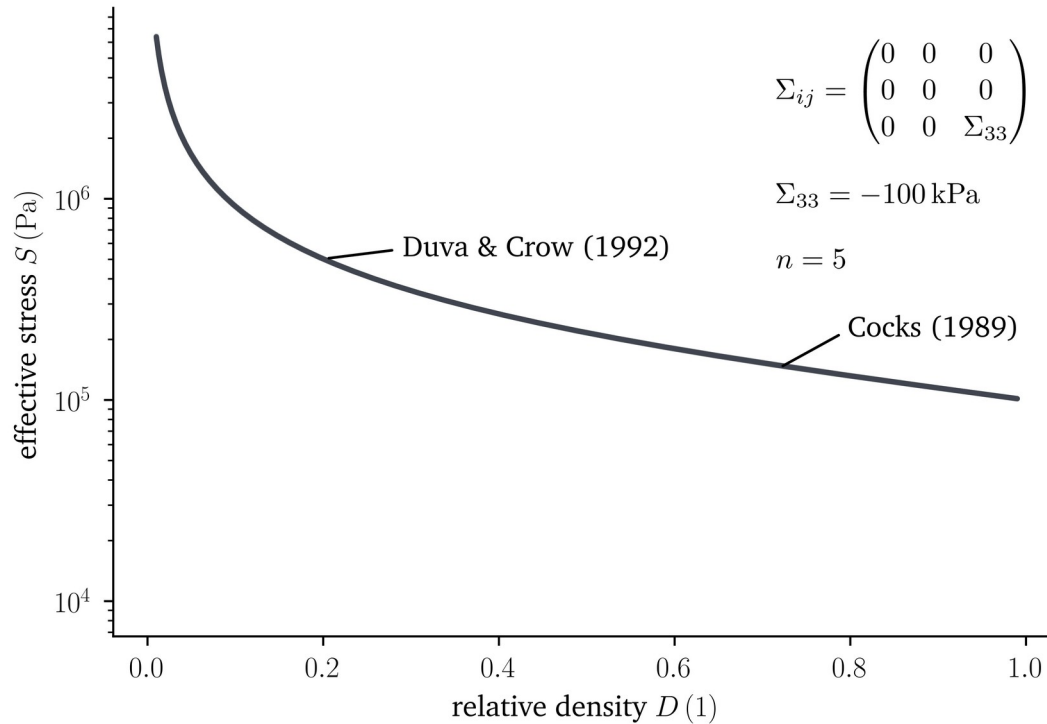
Duva and Crow (1994)



Wilkinson and Ashby (1975)

Cocks (1989)

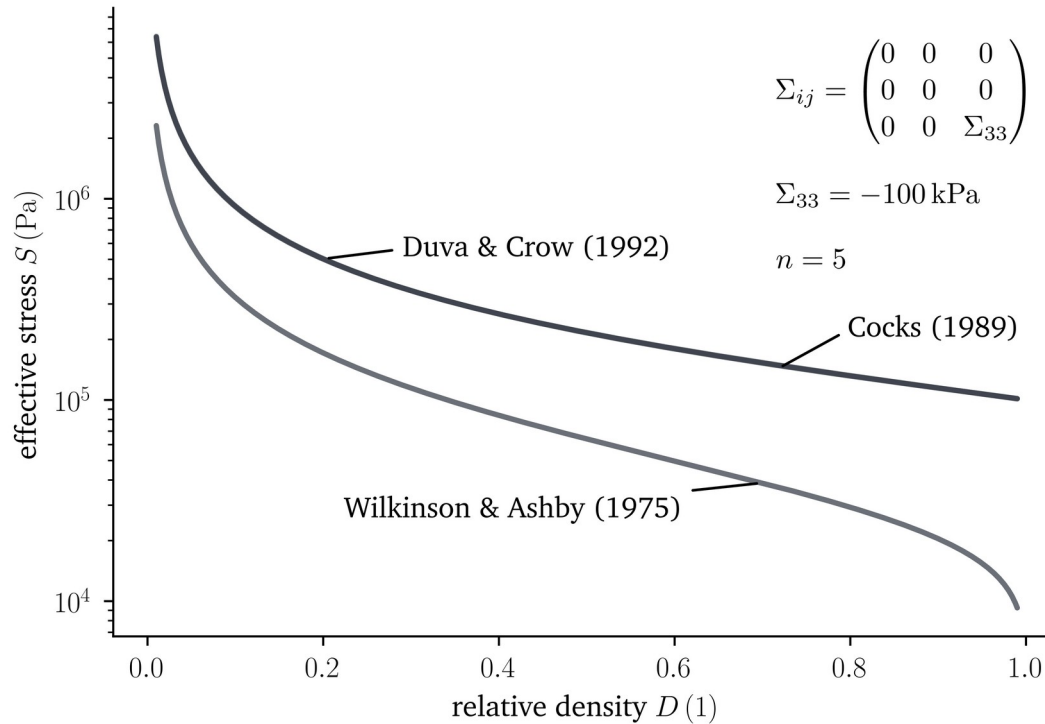
Duva and Crow (1994)



Wilkinson and Ashby (1975)

Cocks (1989)

Duva and Crow (1994)



Wilkinson and Ashby (1975)

Cocks (1989)

Duva and Crow (1994)

$$\dot{E}_{ij} = \frac{\partial \tilde{\Psi}}{\partial \Sigma_{ij}}$$

$$\tilde{\Psi} = \frac{1}{(n+1)} B^* S^{(n+1)}$$

flow potential

$$S = \left(a(\rho) \Sigma_e^2 + b(\rho) \Sigma_m^2 \right)^{\frac{1}{2}}$$

effective stress

$$\dot{E}_{ij} = \frac{1}{2} B^*(T) \left(a(\rho) \Sigma_e^2 + b(\rho) \Sigma_m^2 \right)^{\frac{(n-1)}{2}} \left(3a(\rho) \Sigma_{ij}^D + \frac{2}{3} b(\rho) \Sigma_m \right)$$

stress form

$$\Sigma_{ij} = \frac{\partial \Psi}{\partial \dot{E}_{ij}}$$

$$\Psi = \frac{n}{(n+1)} B^* - \frac{1}{n} E^{\frac{(n+1)}{n}}$$

strain energy rate density

$$E = \left(\frac{1}{a(\rho)} \dot{E}_e^2 + \frac{1}{b(\rho)} \dot{E}_m^2 \right)^{\frac{1}{2}}$$

effective strain rate

$$\Sigma_{ij} = \frac{1}{2} B^* (T)^{-\frac{1}{n}} \left(\frac{1}{a(\rho)} \dot{E}_e^2 + \frac{1}{b(\rho)} \dot{E}_m^2 \right)^{\frac{(1-n)}{2n}} \left(\frac{4}{3a(\rho)} \dot{e}_{ij} + \frac{2}{b(\rho)} \dot{E}_m \right)$$

with $\dot{E}_e^2 = \frac{2}{3} \dot{e}_{ij} \dot{e}_{ij}$ $\dot{E}_m = \dot{E}_{kk}$ $\dot{e}_{ij} = \dot{E}_{ij} - \frac{1}{3} \dot{E}_{kk} \delta_{ij}$

strain rate form
interpretation

$$\Sigma_{ij} = \frac{1}{2} B^*(T)^{-\frac{1}{n}} \left(\frac{1}{a(\rho)} \dot{E}_e^2 + \frac{1}{b(\rho)} \dot{E}_m^2 \right)^{\frac{(1-n)}{2n}} \left(\frac{4}{3 a(\rho)} \dot{e}_{ij} + \frac{2}{b(\rho)} \dot{E}_m \right)$$

stress form

$$\Sigma_{ij} = \frac{2}{3 a(\rho)} B^*(T)^{-\frac{1}{n}} E(\rho, \dot{E}_{ij})^{\frac{(1-n)}{n}} \dot{e}_{ij} + \frac{1}{b(\rho)} B^*(T)^{-\frac{1}{n}} E(\rho, \dot{E}_{ij})^{\frac{(1-n)}{n}} \dot{E}_m$$

$$\boldsymbol{\sigma} = -p(\rho, T) \mathbf{1} + 2\eta(\rho, T) \dot{\boldsymbol{\epsilon}}^D + (\zeta(\rho, T) \operatorname{tr}(\dot{\boldsymbol{\epsilon}})) \mathbf{1}$$

Haupt, P. (2000). *Continuum Mechanics and Theory of Materials*. Advanced Texts in Physics. Berlin, Heidelberg: Springer-Verlag. ISBN: 978-3-662-04109-3.

Greve, R. and Blatter, H. (2009). *Dynamics of Ice Sheets and Glaciers*. Ed. by Hutter, K. Advances in Geophysical and Environmental Mechanics and Mathematics. Berlin, Heidelberg: Springer. ISBN: 978-3-642-03414-5.

stress form

$$\Sigma_{ij} = \frac{2}{3 a(\rho)} B^*(T)^{-\frac{1}{n}} E \left(\rho, \dot{E}_{ij} \right)^{\frac{(1-n)}{n}} \dot{e}_{ij} + \frac{1}{b(\rho)} B^*(T)^{-\frac{1}{n}} E \left(\rho, \dot{E}_{ij} \right)^{\frac{(1-n)}{n}} \dot{E}_m$$

shear viscosity

$$\boldsymbol{\sigma} = -p(\rho, T) \mathbf{1} + 2\eta(\rho, T) \dot{\boldsymbol{\epsilon}}^D + (\zeta(\rho, T) \text{tr}(\dot{\boldsymbol{\epsilon}})) \mathbf{1}$$

$$\eta(\rho, T, \dot{E}_{ij}) = \frac{1}{3 a(\rho)} B^*(T)^{-\frac{1}{n}} \left(\frac{1}{a(\rho)} \dot{E}_e^2 + \frac{1}{b(\rho)} \dot{E}_m^2 \right)^{\frac{(1-n)}{2n}}$$

Haupt, P. (2000). *Continuum Mechanics and Theory of Materials*. Advanced Texts in Physics. Berlin, Heidelberg: Springer-Verlag. ISBN: 978-3-662-04109-3.

Greve, R. and Blatter, H. (2009). *Dynamics of Ice Sheets and Glaciers*. Ed. by Hutter, K. Advances in Geophysical and Environmental Mechanics and Mathematics. Berlin, Heidelberg: Springer. ISBN: 978-3-642-03414-5.

stress form

$$\Sigma_{ij} = \frac{2}{3 a(\rho)} B^*(T)^{-\frac{1}{n}} E \left(\rho, \dot{E}_{ij} \right)^{\frac{(1-n)}{n}} \dot{e}_{ij} + \boxed{\frac{1}{b(\rho)} B^*(T)^{-\frac{1}{n}} E \left(\rho, \dot{E}_{ij} \right)^{\frac{(1-n)}{n}} \dot{E}_m}$$

bulk viscosity

$$\boldsymbol{\sigma} = -p(\rho, T) \mathbf{1} + 2\eta(\rho, T) \dot{\boldsymbol{\varepsilon}}^D + (\zeta(\rho, T) \operatorname{tr}(\dot{\boldsymbol{\varepsilon}})) \mathbf{1}$$

$$\zeta \left(\rho, T, \dot{E}_{ij} \right) = \frac{1}{b(\rho)} B^*(T)^{-\frac{1}{n}} \left(\frac{1}{a(\rho)} \dot{E}_e^2 + \frac{1}{b(\rho)} \dot{E}_m^2 \right)^{\frac{(1-n)}{2n}}$$

Haupt, P. (2000). *Continuum Mechanics and Theory of Materials*. Advanced Texts in Physics. Berlin, Heidelberg: Springer-Verlag. ISBN: 978-3-662-04109-3.

Greve, R. and Blatter, H. (2009). *Dynamics of Ice Sheets and Glaciers*. Ed. by Hutter, K. Advances in Geophysical and Environmental Mechanics and Mathematics. Berlin, Heidelberg: Springer. ISBN: 978-3-642-03414-5.

stress form

$$\Sigma_{ij} = \frac{2}{3 a(\rho)} B^*(T)^{-\frac{1}{n}} E \left(\rho, \dot{E}_{ij} \right)^{\frac{(1-n)}{n}} \dot{e}_{ij} + \frac{1}{b(\rho)} B^*(T)^{-\frac{1}{n}} E \left(\rho, \dot{E}_{ij} \right)^{\frac{(1-n)}{n}} \dot{E}_m$$

shear viscosity

bulk viscosity

$$\boldsymbol{\sigma} = -p(\rho, T) \mathbf{1} + 2\eta(\rho, T) \dot{\boldsymbol{\epsilon}}^D + (\zeta(\rho, T) \text{tr}(\dot{\boldsymbol{\epsilon}})) \mathbf{1}$$

$$\eta(\rho, T, \dot{E}_{ij}) = \frac{1}{3 a(\rho)} B^*(T)^{-\frac{1}{n}} \left(\frac{1}{a(\rho)} \dot{E}_e^2 + \frac{1}{b(\rho)} \dot{E}_m^2 \right)^{\frac{(1-n)}{2n}}$$

$$\zeta(\rho, T, \dot{E}_{ij}) = \frac{1}{b(\rho)} B^*(T)^{-\frac{1}{n}} \left(\frac{1}{a(\rho)} \dot{E}_e^2 + \frac{1}{b(\rho)} \dot{E}_m^2 \right)^{\frac{(1-n)}{2n}}$$

Haupt, P. (2000). *Continuum Mechanics and Theory of Materials*. Advanced Texts in Physics. Berlin, Heidelberg: Springer-Verlag. ISBN: 978-3-662-04109-3.

Greve, R. and Blatter, H. (2009). *Dynamics of Ice Sheets and Glaciers*. Ed. by Hutter, K. Advances in Geophysical and Environmental Mechanics and Mathematics. Berlin, Heidelberg: Springer. ISBN: 978-3-642-03414-5.

stress form

$$\Sigma_{ij} = \frac{2}{3 a(\rho)} B^*(T)^{-\frac{1}{n}} E(\rho, \dot{E}_{ij})^{\frac{(1-n)}{n}} \dot{e}_{ij} + \frac{1}{b(\rho)} B^*(T)^{-\frac{1}{n}} E(\rho, \dot{E}_{ij})^{\frac{(1-n)}{n}} \dot{E}_m$$

$$\frac{1}{2} B^*(T)^{-\frac{1}{n}} \left(\frac{1}{a_{\text{firm}}(\rho)} \dot{E}_e^2 + \frac{1}{b_{\text{firm}}(\rho)} \dot{E}_m^2 \right)^{\frac{(1-n)}{2n}} \left(\frac{4}{3a_{\text{firm}}(\rho)} \dot{e}_{zz} + \frac{2}{b_{\text{firm}}(\rho)} \dot{E}_m \right) - \Sigma_{zz} = 0$$

to be determined

a_{firm} parameter a

b_{firm} parameter b

unknowns

\dot{E}_{ij} strain rate tensor

Σ_{zz} vertical stress

T temperature

ρ density

$$\frac{1}{2} B^*(T)^{-\frac{1}{n}} \left(\frac{1}{a_{\text{firm}}(\rho)} \dot{E}_e^2 + \frac{1}{b_{\text{firm}}(\rho)} \dot{E}_m^2 \right)^{\frac{(1-n)}{2n}} \left(\frac{4}{3a_{\text{firm}}(\rho)} \dot{e}_{zz} + \frac{2}{b_{\text{firm}}(\rho)} \dot{E}_m \right) - \Sigma_{zz} = 0$$

to be determined

a_{firm} parameter a

b_{firm} parameter b

unknowns

\dot{E}_{ij} strain rate tensor

Σ_{zz} vertical stress

T temperature

ρ density

$$\frac{1}{2} B^*(T)^{-\frac{1}{n}} \left(\frac{1}{a_{\text{firm}}(\rho)} \dot{E}_e^2 + \frac{1}{b_{\text{firm}}(\rho)} \dot{E}_m^2 \right)^{\frac{(1-n)}{2n}} \left(\frac{4}{3a_{\text{firm}}(\rho)} \dot{e}_{zz} + \frac{2}{b_{\text{firm}}(\rho)} \dot{E}_m \right) - \Sigma_{zz} = 0$$

to be determined

a_{firm} parameter a

b_{firm} parameter b

unknowns

\dot{E}_{ij} strain rate tensor

Σ_{zz} vertical stress

T temperature

ρ density

$$\frac{1}{2} B^*(T)^{-\frac{1}{n}} \left(\frac{1}{a_{\text{firm}}(\rho)} \dot{E}_e^2 + \frac{1}{b_{\text{firm}}(\rho)} \dot{E}_m^2 \right)^{\frac{(1-n)}{2n}} \left(\frac{4}{3a_{\text{firm}}(\rho)} \dot{e}_{zz} + \frac{2}{b_{\text{firm}}(\rho)} \dot{E}_m \right) - \Sigma_{zz} = 0$$

to be determined

a_{firm} parameter a

b_{firm} parameter b

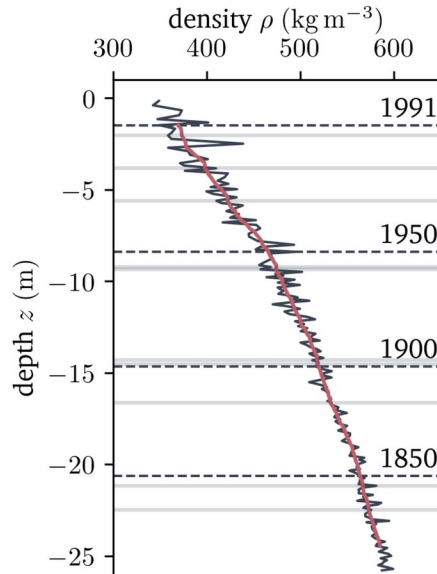
unknowns

\dot{E}_{ij} strain rate tensor

Σ_{zz} vertical stress

T temperature

ρ density

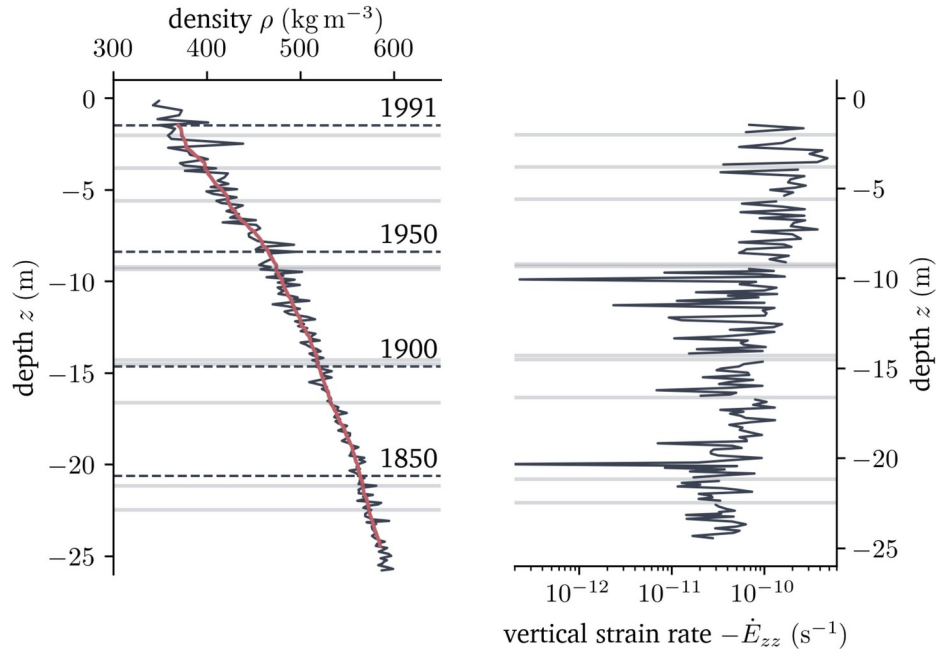


local form of the mass balance

$$\frac{\partial \rho}{\partial t} = -\rho \left(\frac{\partial v_x}{\partial x} + \frac{\partial v_y}{\partial y} + \frac{\partial v_z}{\partial z} \right)$$

Oerter, H. F., Wilhelms, F., Jung-Rothehäusler, F., Götka, F., Miller, H., Graf, W., and Sommer, S. (2000). *Physical Properties of firn core DML05C98_07*. PANGAEA.

Graf, W., Oerter, H., Reinwarth, O., Stichler, W., Wilhelms, F., Miller, H., and Mulvaney, R. (2002). *Calculated annual mean of d_{18O} of firn core DML05C98_07*. PANGAEA. <https://doi.org/https://doi.org/10.1594/PANGAEA.104880>



local form of the mass balance

$$\frac{\partial \rho}{\partial t} = -\rho \left(\frac{\partial v_x}{\partial x} + \frac{\partial v_y}{\partial y} + \frac{\partial v_z}{\partial z} \right)$$

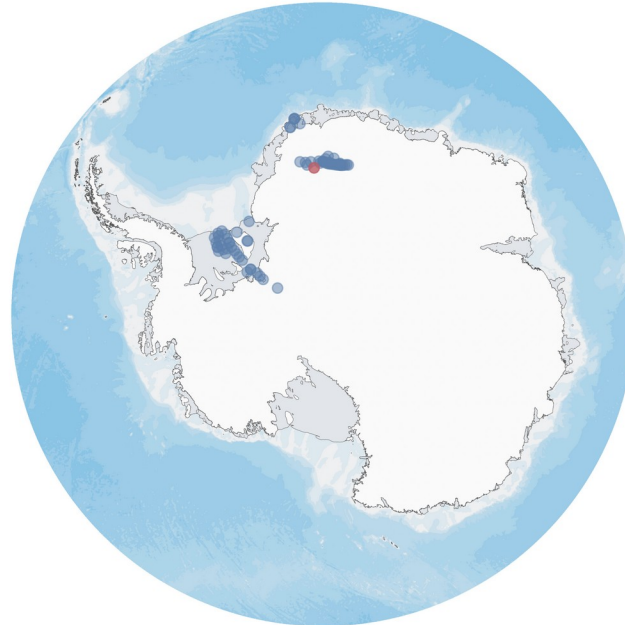
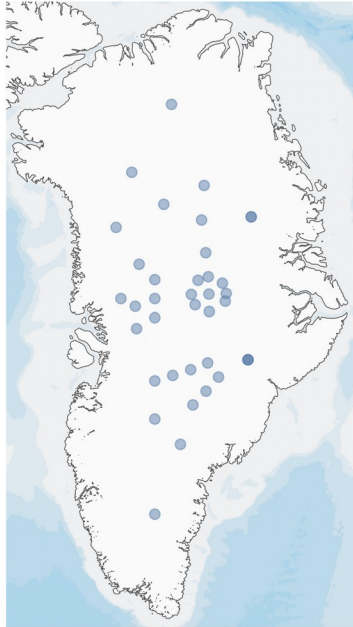
$$\dot{\tilde{E}}_{zz} = -\frac{1}{\rho} \frac{\partial \rho}{\partial t} - \dot{\tilde{E}}_{xx} - \dot{\tilde{E}}_{yy}$$

$$\dot{\tilde{E}}_{zz}^n = -\frac{1}{\rho_i^n} \frac{(\rho_{i+1}^{n+1} - \rho_i^n)}{(\chi_{i+1}^{n+1} - \chi_i^n)} - \dot{\tilde{E}}_{xx} - \dot{\tilde{E}}_{yy}$$

Oerter, H. F., Wilhelms, F., Jung-Rothehäusler, F., Götkaas, F., Miller, H., Graf, W., and Sommer, S. (2000). *Physical Properties of firn core DML05C98_07*. PANGAEA.

Graf, W., Oerter, H., Reinwarth, O., Stichler, W., Wilhelms, F., Miller, H., and Mulvaney, R. (2002). *Calculated annual mean of $d18\text{O}$ of firn core DML05C98_07*. PANGAEA. <https://doi.org/https://doi.org/10.1594/PANGAEA.104880>

Model Inversion – Cores



Greenland: 38 firn cores

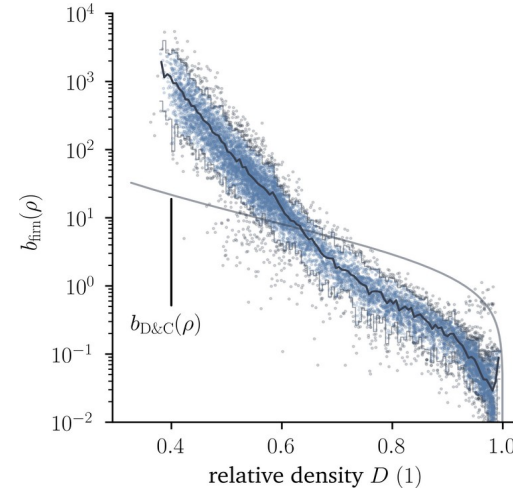
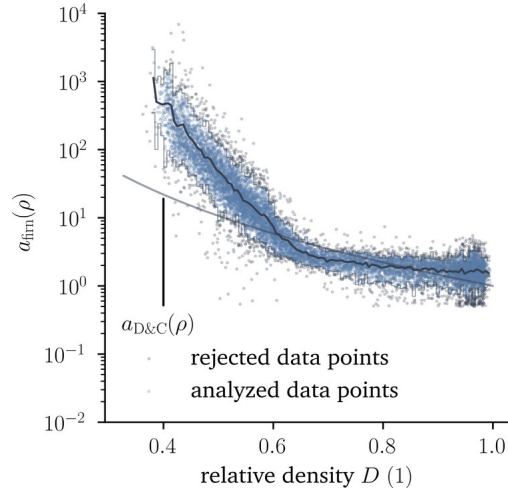
Antarctica: 52 firn cores

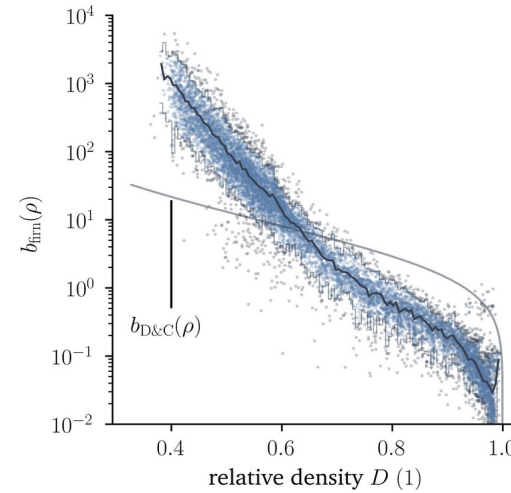
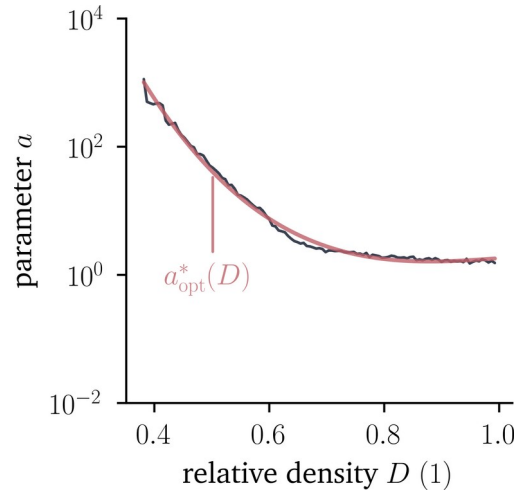
Amante, C. and Eakins, B. W. (2009). *ETOPO1 1 Arc-Minute Global Relief Model: Procedures Data Source, and Analysis*. NOAA Technical Memorandum NESDIS NGDC 24. National Geophysical Data Center, NOAA. <https://repository.library.noaa.gov/view/noaa/1163>

Arndt, J. E., Schenke, H. W., Jakobsson, M., Nitsche, F. O., Buys, G., Goleby, B., Rebesco, M., Bohoyo, F., Hong, J., Black, J., Greku, R., Udintsev, G., Brrios, F., Reynoso-Peralta, W., Taisei, M., and Wigley, R. (2013). *The International Bathymetric Chart of the Southern Ocean (IBSCO) Version 1.0 – A new bathymetric compilation covering circum-Antarctic waters*. *Geophysical Research Letters*, 40(12). pp. 3111-3117. <https://doi.org/https://doi.org/10.1002/grl.50413>

Parameter Determination

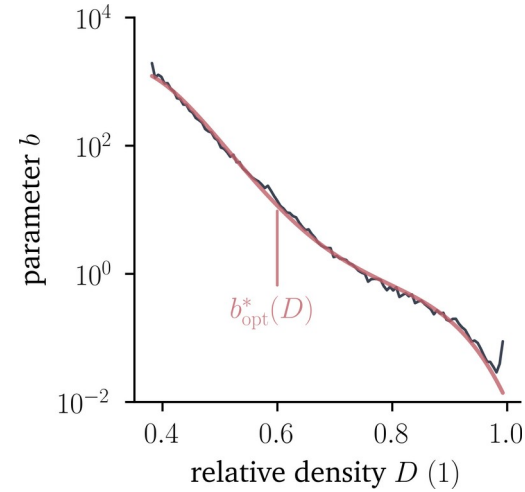
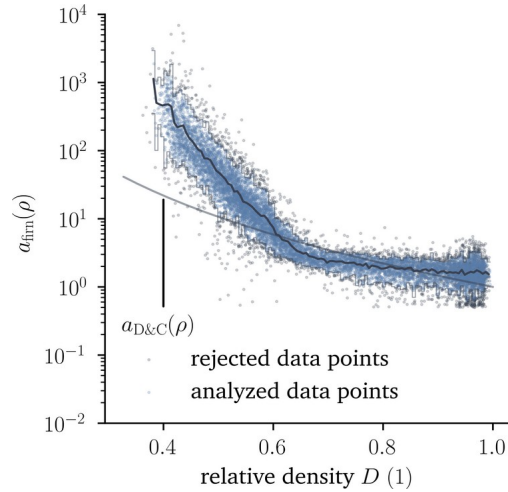
Model Inversion – Parameter Determination





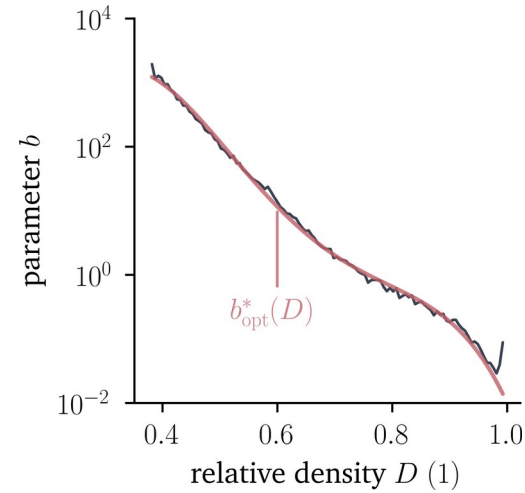
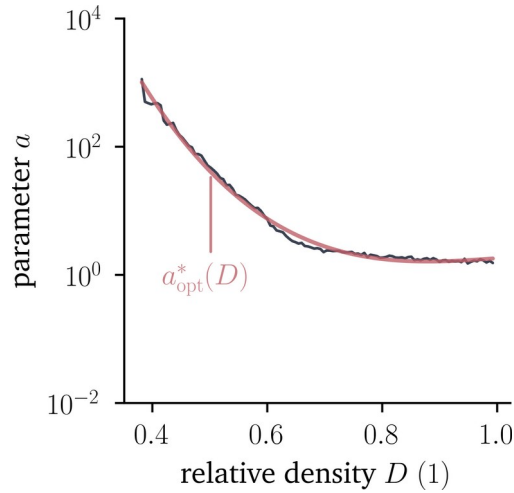
$$\log_{10} (a_{\text{opt}}^* (D)) = a_0 D^3 + a_1 D^2 + a_2 D + a_3$$

$$a_0 = -12.60, \quad a_1 = 38.26, \quad a_2 = -38.06, \quad a_3 = 12.66$$



$$\log_{10} (b_{\text{opt}}^*(D)) = b_0 (D^4 - 1) + b_1 (D^3 - 1) + b_2 (D^2 - 1) + b_3 (D - 1) - 2$$

$$b_0 = -142.96, \quad b_1 = 374.45, \quad b_2 = -351.10, \quad b_3 = 131.26$$



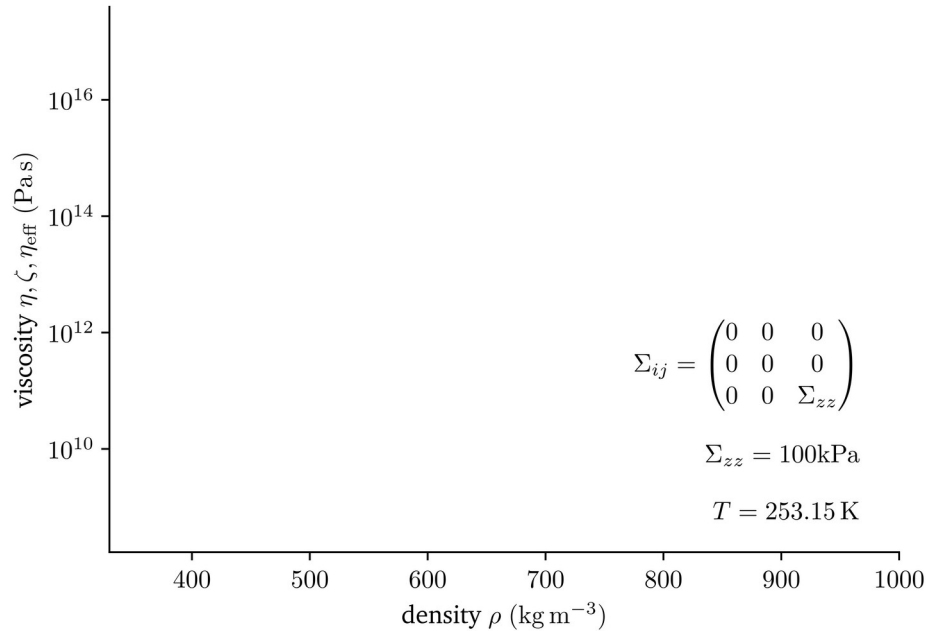
$$\log_{10} (a_{\text{opt}}^* (D)) = a_0 D^3 + a_1 D^2 + a_2 D + a_3$$

$$\log_{10} (b_{\text{opt}}^* (D)) = b_0 (D^4 - 1) + b_1 (D^3 - 1) + b_2 (D^2 - 1) + b_3 (D - 1) - 2$$

$$a_0 = -12.60, \quad a_1 = 38.26, \quad a_2 = -38.06, \quad a_3 = 12.66$$

$$b_0 = -142.96, \quad b_1 = 374.45, \quad b_2 = -351.10, \quad b_3 = 131.26$$

Resulting Material Behavior

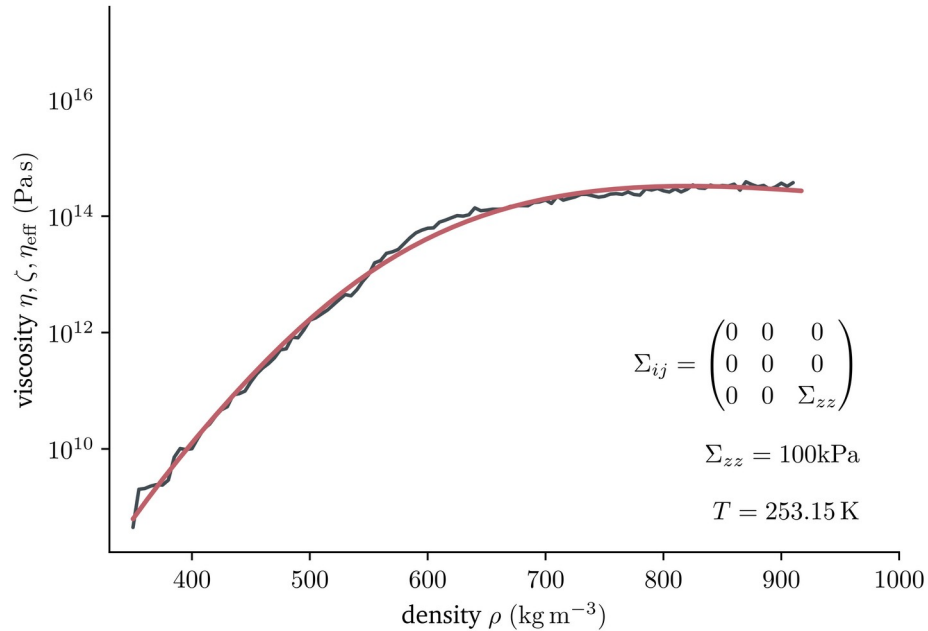


— $\eta(\rho, T, \Sigma_{ij}) = \frac{1}{3a(\rho)} B^*(T)^{-1} (a(\rho) \Sigma_e^2 + b(\rho) \Sigma_m^2)^{\frac{(1-n)}{2}}$

— $\zeta(\rho, T, \Sigma_{ij}) = \frac{1}{b(\rho)} B^*(T)^{-1} (a(\rho) \Sigma_e^2 + b(\rho) \Sigma_m^2)^{\frac{(1-n)}{2}}$

--- η_{ice}

Resulting Material Behavior

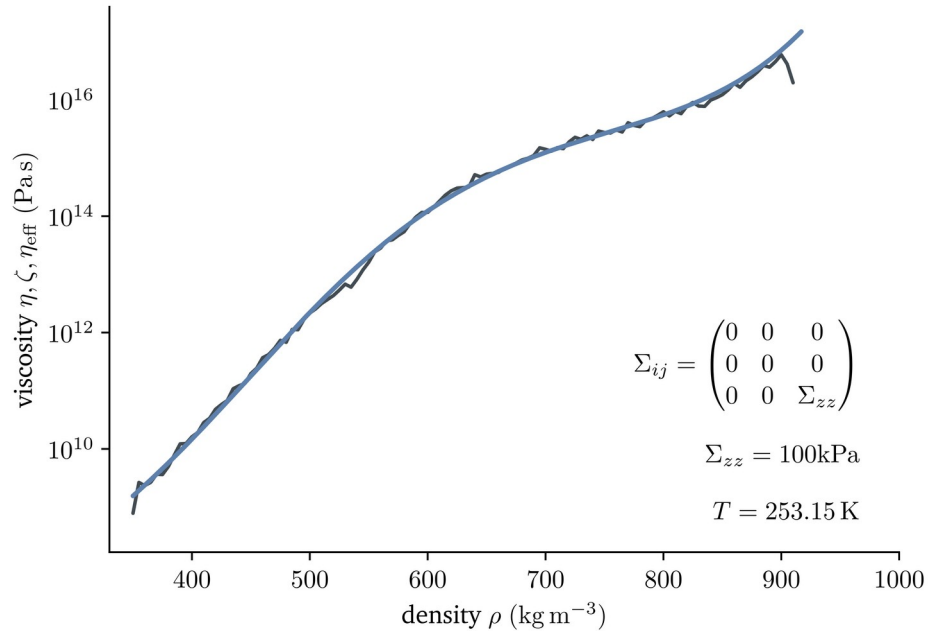


— $\eta(\rho, T, \Sigma_{ij}) = \frac{1}{3a(\rho)} B^*(T)^{-1} (a(\rho) \Sigma_e^2 + b(\rho) \Sigma_m^2)^{\frac{(1-n)}{2}}$

— $\zeta(\rho, T, \Sigma_{ij}) = \frac{1}{b(\rho)} B^*(T)^{-1} (a(\rho) \Sigma_e^2 + b(\rho) \Sigma_m^2)^{\frac{(1-n)}{2}}$

--- η_{ice}

Resulting Material Behavior

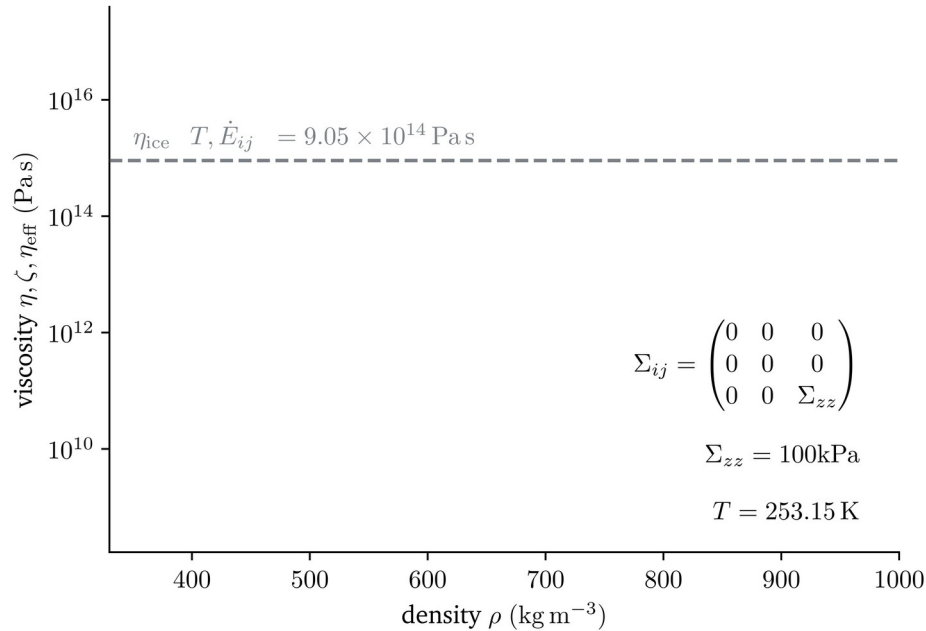


— $\eta(\rho, T, \Sigma_{ij}) = \frac{1}{3a(\rho)} B^*(T)^{-1} (a(\rho) \Sigma_e^2 + b(\rho) \Sigma_m^2)^{\frac{(1-n)}{2}}$

— $\zeta(\rho, T, \Sigma_{ij}) = \frac{1}{b(\rho)} B^*(T)^{-1} (a(\rho) \Sigma_e^2 + b(\rho) \Sigma_m^2)^{\frac{(1-n)}{2}}$

--- η_{ice}

Resulting Material Behavior

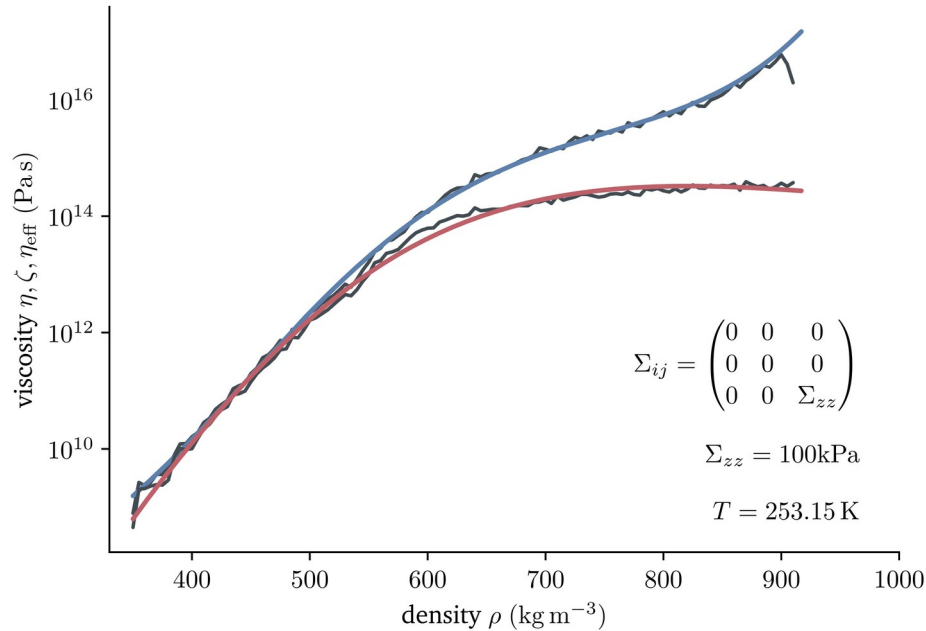


$$\eta(\rho, T, \Sigma_{ij}) = \frac{1}{3a(\rho)} B^*(T)^{-1} (a(\rho) \Sigma_e^2 + b(\rho) \Sigma_m^2)^{\frac{(1-n)}{2}}$$

$$\zeta(\rho, T, \Sigma_{ij}) = \frac{1}{b(\rho)} B^*(T)^{-1} (a(\rho) \Sigma_e^2 + b(\rho) \Sigma_m^2)^{\frac{(1-n)}{2}}$$

--- η_{ice}

Resulting Material Behavior

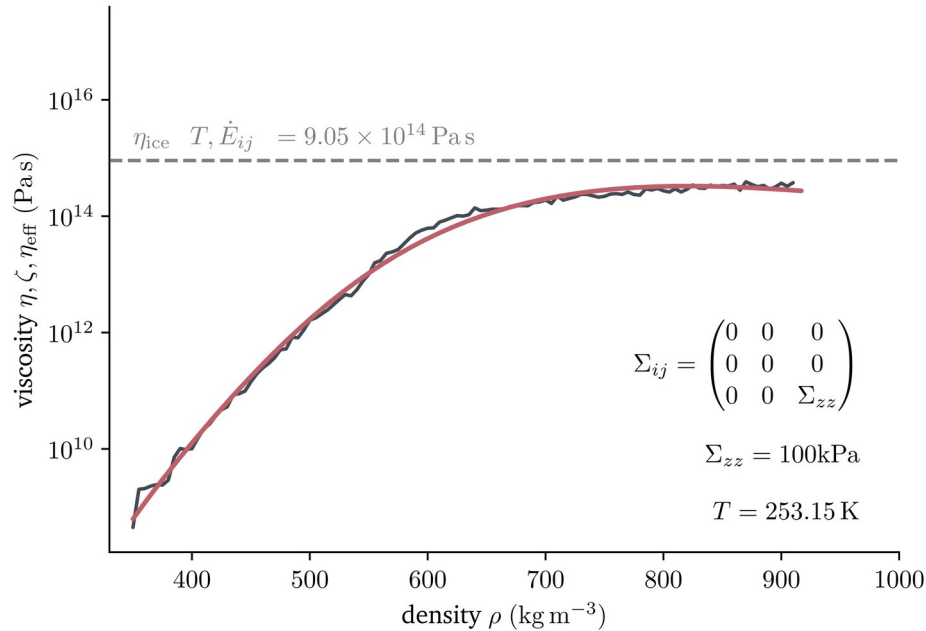


— $\eta(\rho, T, \Sigma_{ij}) = \frac{1}{3a(\rho)} B^*(T)^{-1} (a(\rho) \Sigma_e^2 + b(\rho) \Sigma_m^2)^{\frac{(1-n)}{2}}$

— $\zeta(\rho, T, \Sigma_{ij}) = \frac{1}{b(\rho)} B^*(T)^{-1} (a(\rho) \Sigma_e^2 + b(\rho) \Sigma_m^2)^{\frac{(1-n)}{2}}$

--- η_{ice}

Resulting Material Behavior

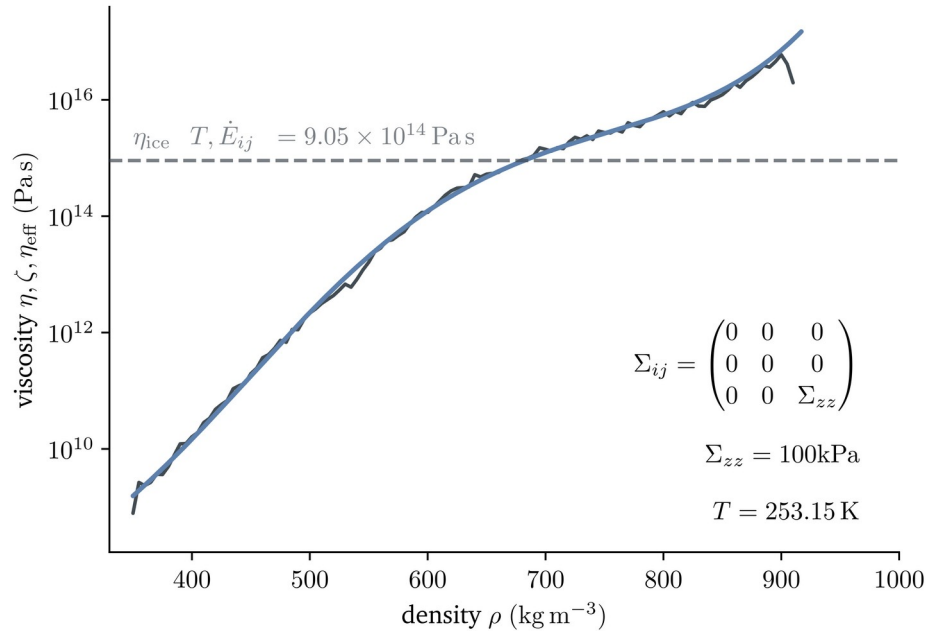


— $\eta(\rho, T, \Sigma_{ij}) = \frac{1}{3a(\rho)} B^*(T)^{-1} (a(\rho) \Sigma_e^2 + b(\rho) \Sigma_m^2)^{\frac{(1-n)}{2}}$

— $\zeta(\rho, T, \Sigma_{ij}) = \frac{1}{b(\rho)} B^*(T)^{-1} (a(\rho) \Sigma_e^2 + b(\rho) \Sigma_m^2)^{\frac{(1-n)}{2}}$

--- η_{ice}

Resulting Material Behavior

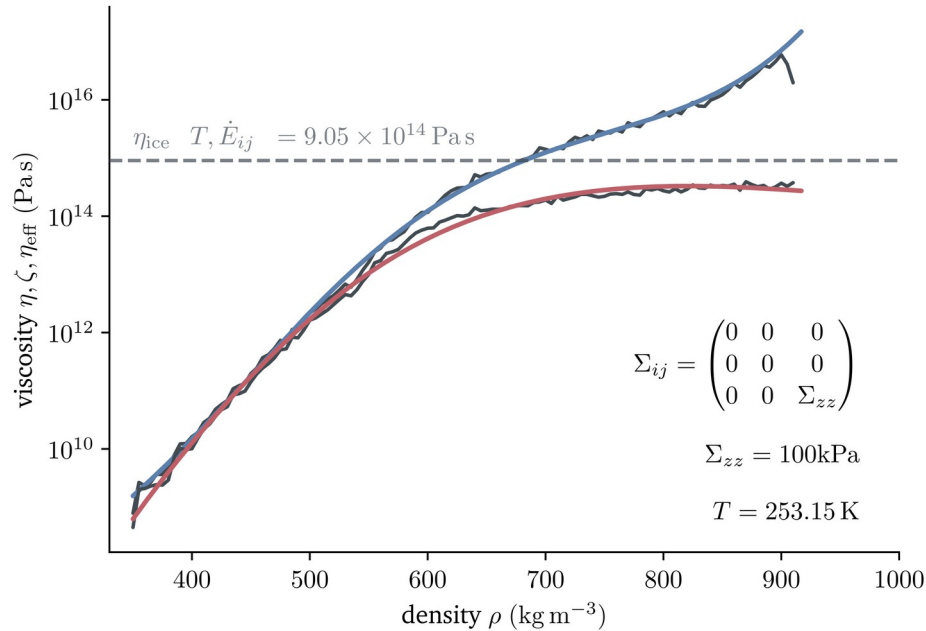


— $\eta(\rho, T, \Sigma_{ij}) = \frac{1}{3a(\rho)} B^*(T)^{-1} (a(\rho) \Sigma_e^2 + b(\rho) \Sigma_m^2)^{\frac{(1-n)}{2}}$

— $\zeta(\rho, T, \Sigma_{ij}) = \frac{1}{b(\rho)} B^*(T)^{-1} (a(\rho) \Sigma_e^2 + b(\rho) \Sigma_m^2)^{\frac{(1-n)}{2}}$

— η_{ice}

Resulting Material Behavior

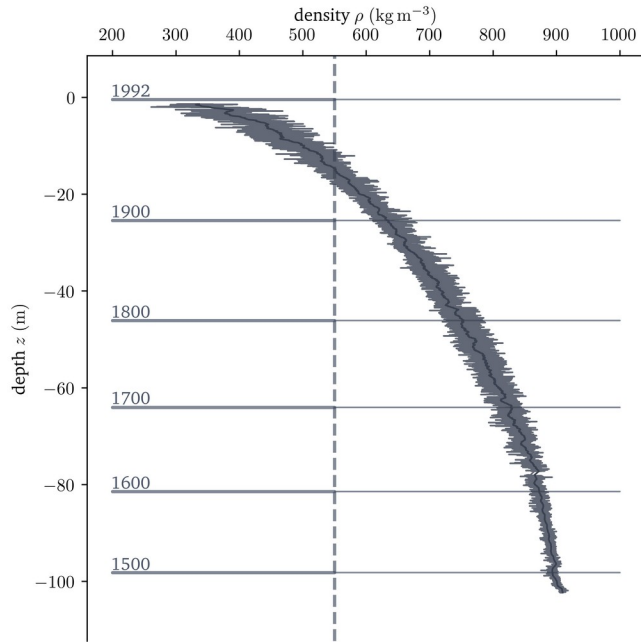


— $\eta(\rho, T, \Sigma_{ij}) = \frac{1}{3a(\rho)} B^*(T)^{-1} (a(\rho) \Sigma_e^2 + b(\rho) \Sigma_m^2)^{\frac{(1-n)}{2}}$

— $\zeta(\rho, T, \Sigma_{ij}) = \frac{1}{b(\rho)} B^*(T)^{-1} (a(\rho) \Sigma_e^2 + b(\rho) \Sigma_m^2)^{\frac{(1-n)}{2}}$

— η_{ice}

Examples - B16

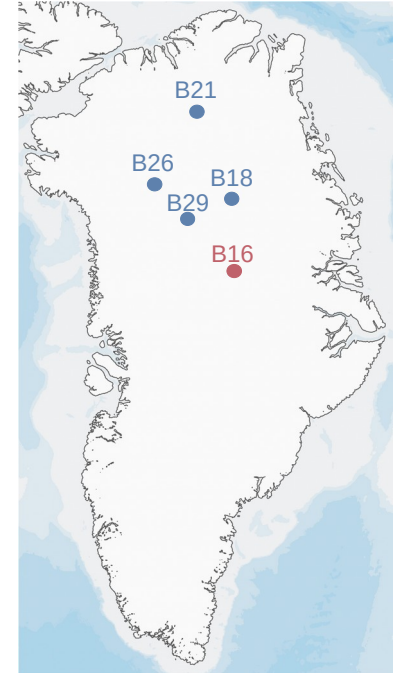


Wilhelms, F. (1996). Density of ice core ngt03C93.2 from the North Greenland Traverse. PANGAEA.

Miller, H. and Schwager, M. (2000). Accumulation rate and stable oxygen isotope ratios of ice core ngt03C93.2 from the North Greenland Traverse. PANGAEA.

— Herron & Langway (1980)

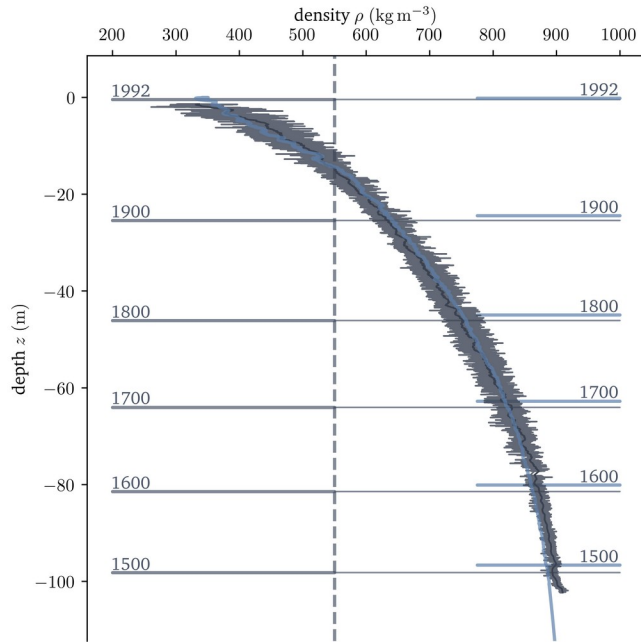
— Cell Model Approach



Amante, C. and Eakins, B. W. (2009). ETOPO1 1 Arc-Minute Global Relief Model: Procedures, Data Source, and Analysis. NOAA.

Arndt, J. E. et al. (2013). The International Bathymetric Chart of the Southern Ocean (IBSCO) Version 1.0 – A new bathymetric compilation covering circum-Antarctic waters. Geophysical Research Letters.

Examples - B16

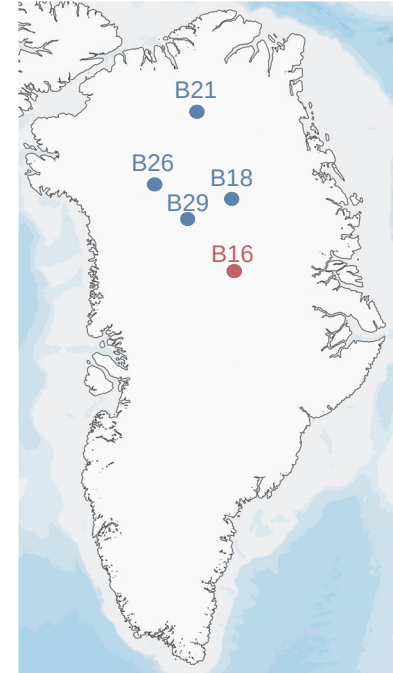


Wilhelms, F. (1996). Density of ice core ngt03C93.2 from the North Greenland Traverse. PANGAEA.

Miller, H. and Schwager, M. (2000). Accumulation rate and stable oxygen isotope ratios of ice core ngt03C93.2 from the North Greenland Traverse. PANGAEA.

— Herron & Langway (1980)

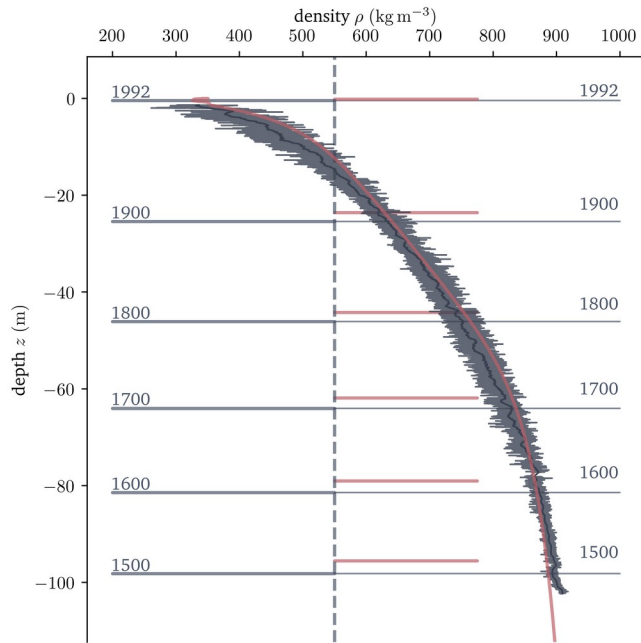
— Cell Model Approach



Amante, C. and Eakins, B. W. (2009). ETOPO1 1 Arc-Minute Global Relief Model: Procedures, Data Source, and Analysis. NOAA.

Arndt, J. E. et al. (2013). The International Bathymetric Chart of the Southern Ocean (IBSCO) Version 1.0 – A new bathymetric compilation covering circum-Antarctic waters. Geophysical Research Letters.

Examples - B16

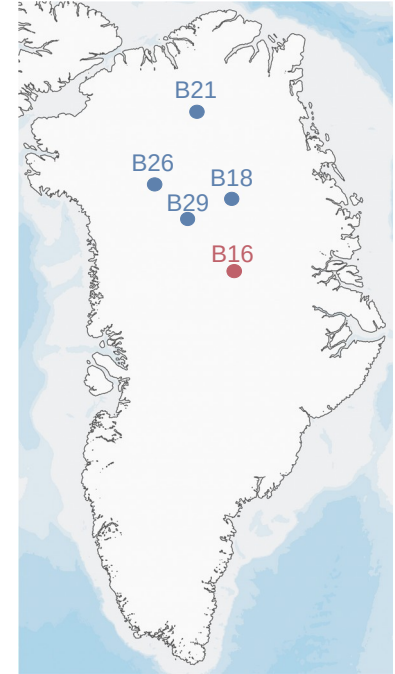


— Herron & Langway (1980)

— Cell Model Approach

Wilhelms, F. (1996). Density of ice core ngt03C93.2 from the North Greenland Traverse. PANGAEA.

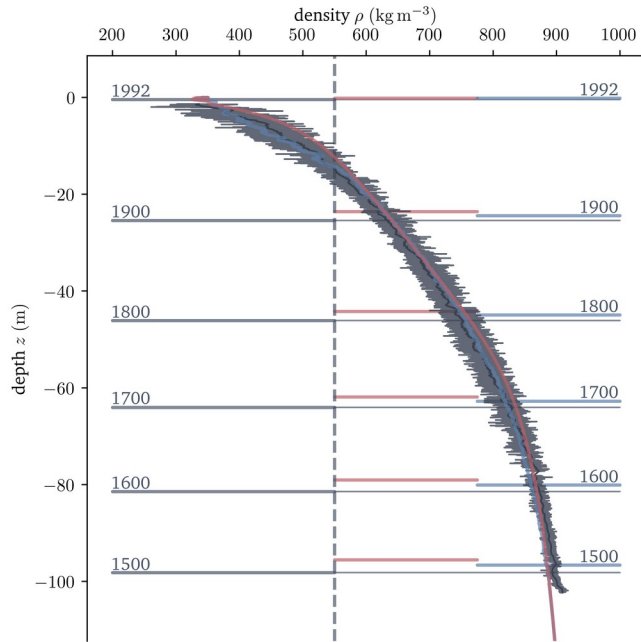
Miller, H. and Schwager, M. (2000). Accumulation rate and stable oxygen isotope ratios of ice core ngt03C93.2 from the North Greenland Traverse. PANGAEA.



Amante, C. and Eakins, B. W. (2009). ETOPO1 1 Arc-Minute Global Relief Model: Procedures, Data Source, and Analysis. NOAA.

Arndt, J. E. et al. (2013). The International Bathymetric Chart of the Southern Ocean (IBSCO) Version 1.0 – A new bathymetric compilation covering circum-Antarctic waters. Geophysical Research Letters.

Examples - B16

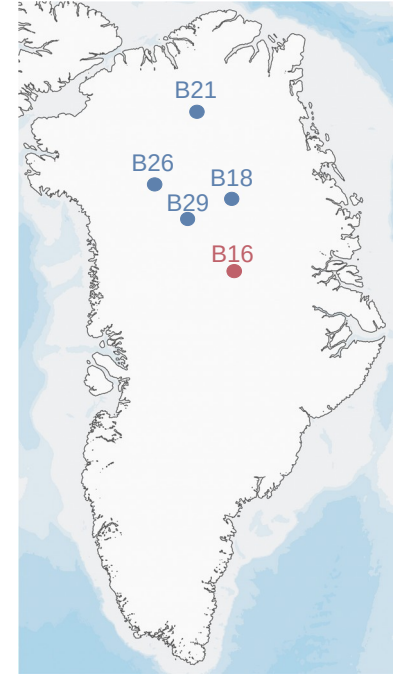


— Herron & Langway (1980)

— Cell Model Approach

Wilhelms, F. (1996). Density of ice core ngt03C93.2 from the North Greenland Traverse. PANGAEA.

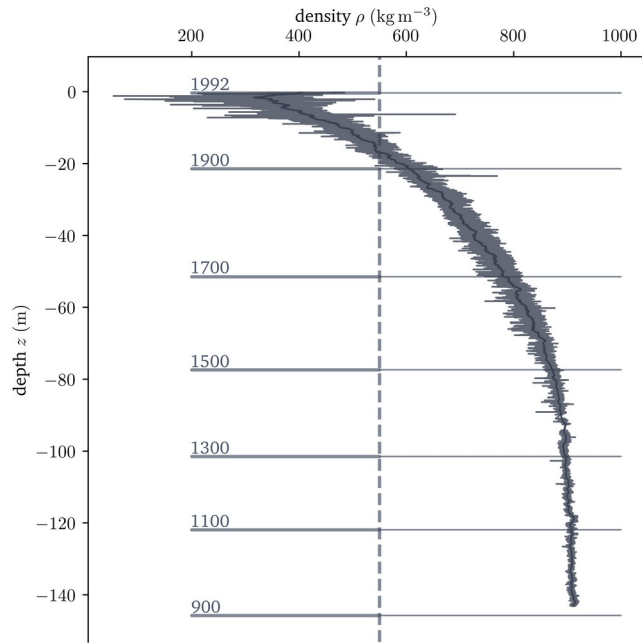
Miller, H. and Schwager, M. (2000). Accumulation rate and stable oxygen isotope ratios of ice core ngt03C93.2 from the North Greenland Traverse. PANGAEA.



Amante, C. and Eakins, B. W. (2009). ETOPO1 1 Arc-Minute Global Relief Model: Procedures, Data Source, and Analysis. NOAA.

Arndt, J. E. et al. (2013). The International Bathymetric Chart of the Southern Ocean (IBSCO) Version 1.0 – A new bathymetric compilation covering circum-Antarctic waters. Geophysical Research Letters.

Examples - B18

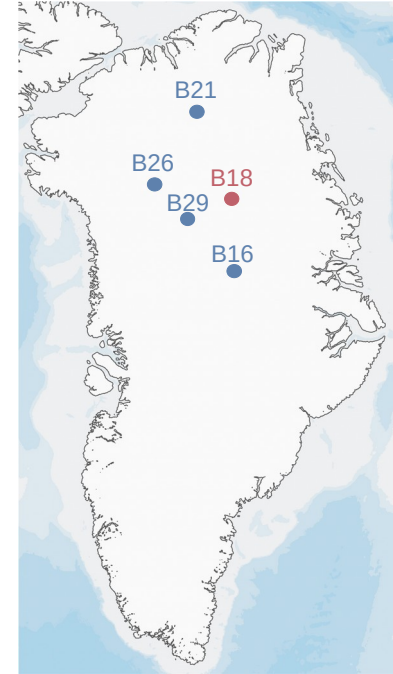


Wilhelms, F. (1996). Density of ice core ngt14C93.2 from the North Greenland Traverse. PANGAEA.

Miller, H. and Schwager, M. (2000). Accumulation rate and stable oxygen isotope ratios of ice core ngt14C93.2 from the North Greenland Traverse. PANGAEA.

— Herron & Langway (1980)

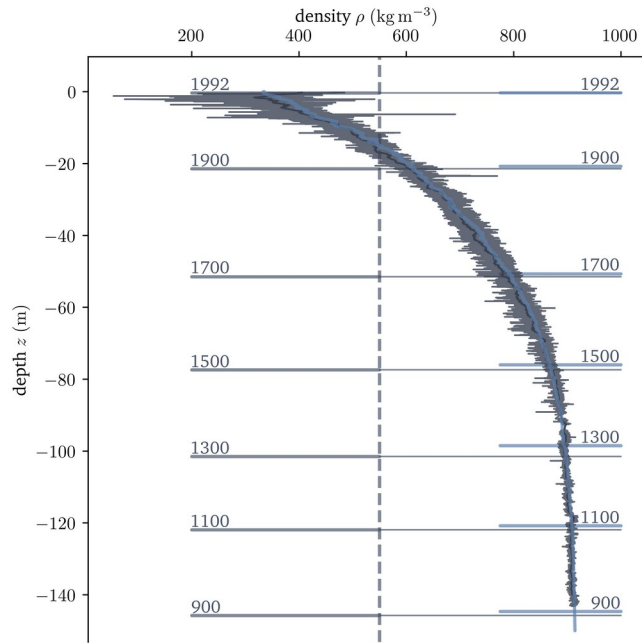
— Cell Model Approach



Amante, C. and Eakins, B. W. (2009). ETOPO1 1 Arc-Minute Global Relief Model: Procedures, Data Source, and Analysis. NOAA.

Arndt, J. E. et al. (2013). The International Bathymetric Chart of the Southern Ocean (IBSCO) Version 1.0 – A new bathymetric compilation covering circum-Antarctic waters. Geophysical Research Letters.

Examples - B18

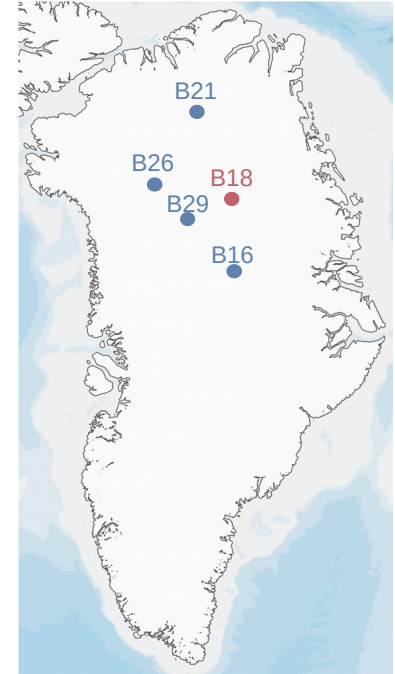


Wilhelms, F. (1996). Density of ice core ngt14C93.2 from the North Greenland Traverse. PANGAEA.

Miller, H. and Schwager, M. (2000). Accumulation rate and stable oxygen isotope ratios of ice core ngt14C93.2 from the North Greenland Traverse. PANGAEA.

— Herron & Langway (1980)

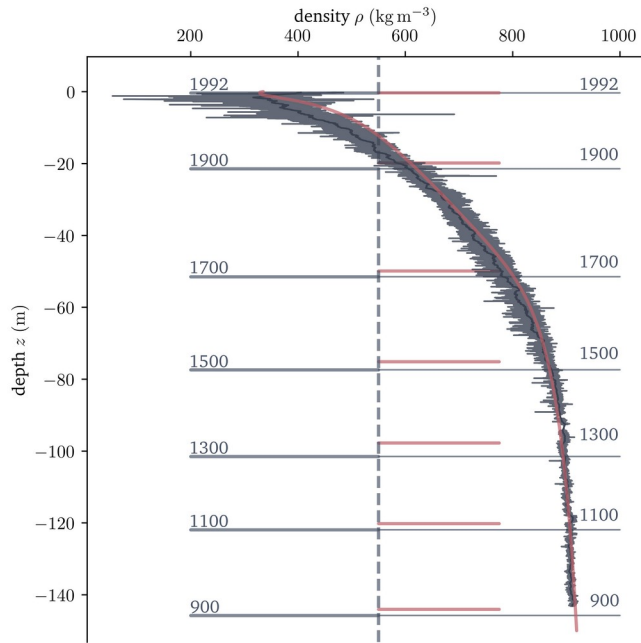
— Cell Model Approach



Amante, C. and Eakins, B. W. (2009). ETOPO1 1 Arc-Minute Global Relief Model: Procedures, Data Source, and Analysis. NOAA.

Arndt, J. E. et al. (2013). The International Bathymetric Chart of the Southern Ocean (IBSCO) Version 1.0 – A new bathymetric compilation covering circum-Antarctic waters. Geophysical Research Letters.

Examples - B18

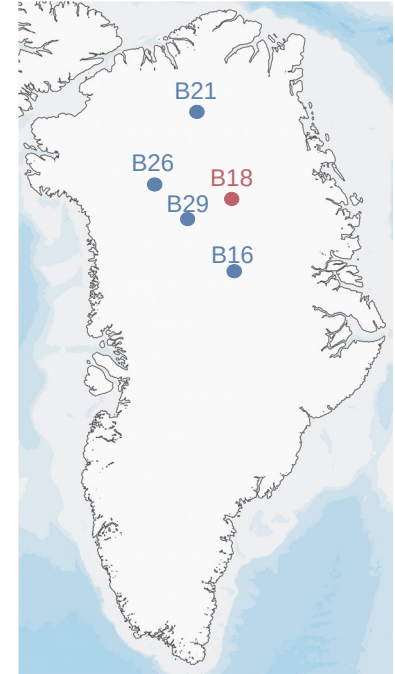


— Herron & Langway (1980)

— Cell Model Approach

Wilhelms, F. (1996). Density of ice core ngt14C93.2 from the North Greenland Traverse. PANGAEA.

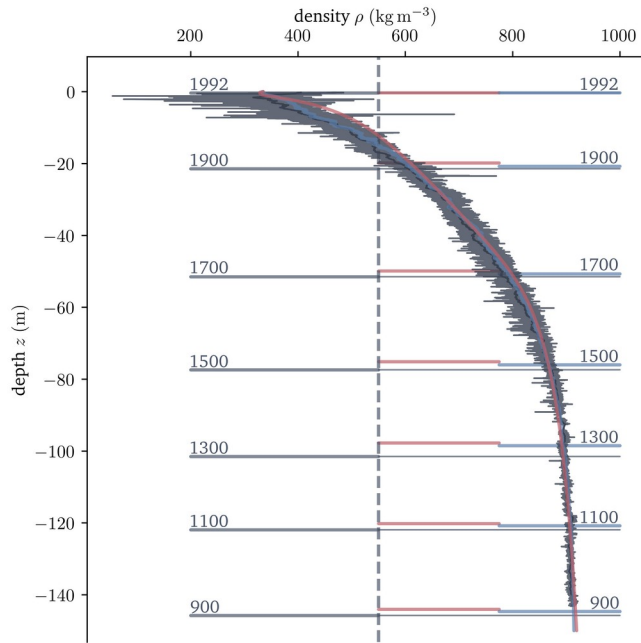
Miller, H. and Schwager, M. (2000). Accumulation rate and stable oxygen isotope ratios of ice core ngt14C93.2 from the North Greenland Traverse. PANGAEA.



Amante, C. and Eakins, B. W. (2009). ETOPO1 1 Arc-Minute Global Relief Model: Procedures, Data Source, and Analysis. NOAA.

Arndt, J. E. et al. (2013). The International Bathymetric Chart of the Southern Ocean (IBSCO) Version 1.0 – A new bathymetric compilation covering circum-Antarctic waters. Geophysical Research Letters.

Examples - B18

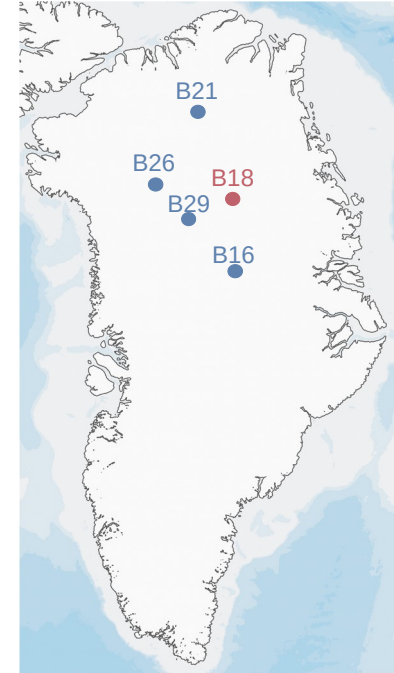


— Herron & Langway (1980)

— Cell Model Approach

Wilhelms, F. (1996). Density of ice core ngt14C93.2 from the North Greenland Traverse. PANGAEA.

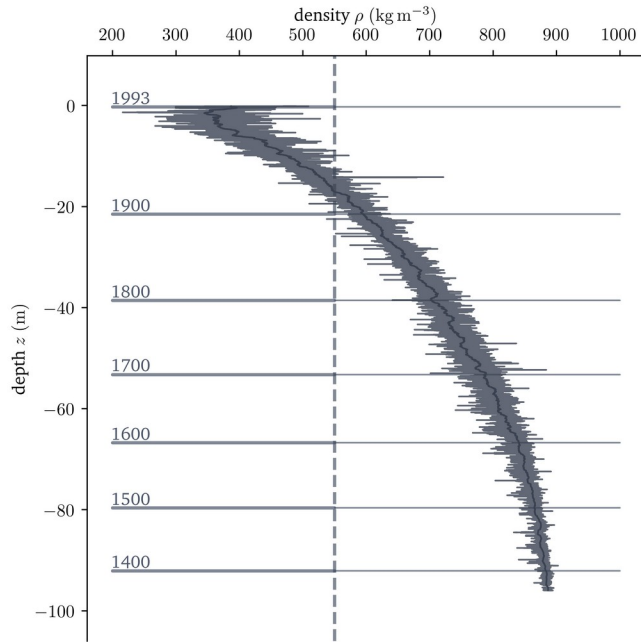
Miller, H. and Schwager, M. (2000). Accumulation rate and stable oxygen isotope ratios of ice core ngt14C93.2 from the North Greenland Traverse. PANGAEA.



Amante, C. and Eakins, B. W. (2009). ETOPO1 1 Arc-Minute Global Relief Model: Procedures, Data Source, and Analysis. NOAA.

Arndt, J. E. et al. (2013). The International Bathymetric Chart of the Southern Ocean (IBSCO) Version 1.0 – A new bathymetric compilation covering circum-Antarctic waters. Geophysical Research Letters.

Examples - B21

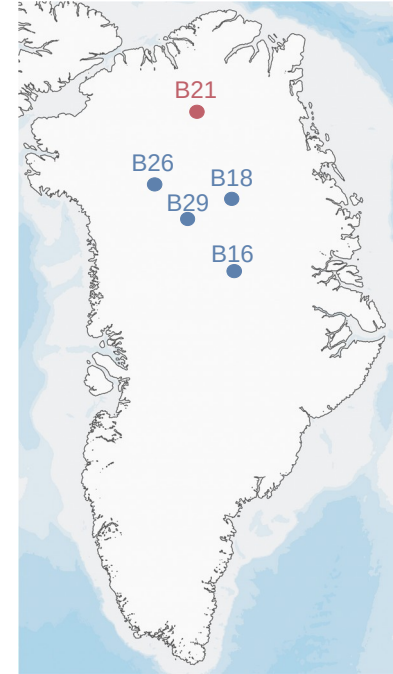


Wilhelms, F. (2000). Density of ice core ngt27C94.2 from the North Greenland Traverse. PANGAEA.

Miller, H. and Schwager, M. (2000). Accumulation rate and stable oxygen isotope ratios of ice core ngt27C94.2 from the North Greenland Traverse. PANGAEA.

— Herron & Langway (1980)

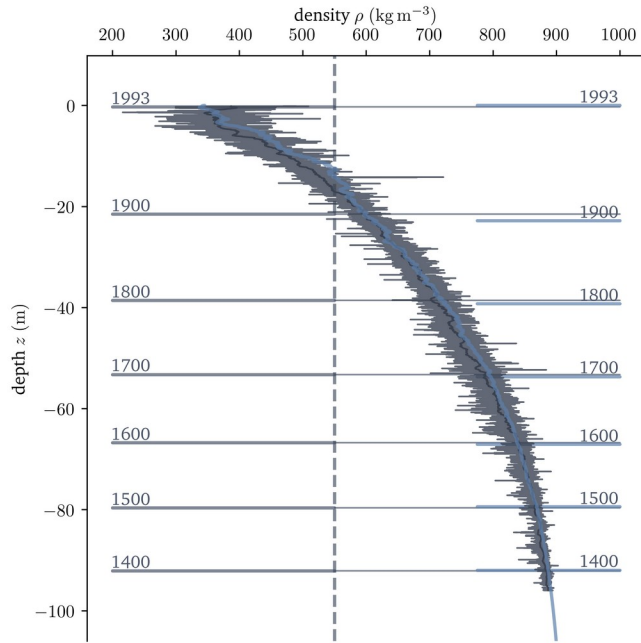
— Cell Model Approach



Amante, C. and Eakins, B. W. (2009). ETOPO1 1 Arc-Minute Global Relief Model: Procedures, Data Source, and Analysis. NOAA.

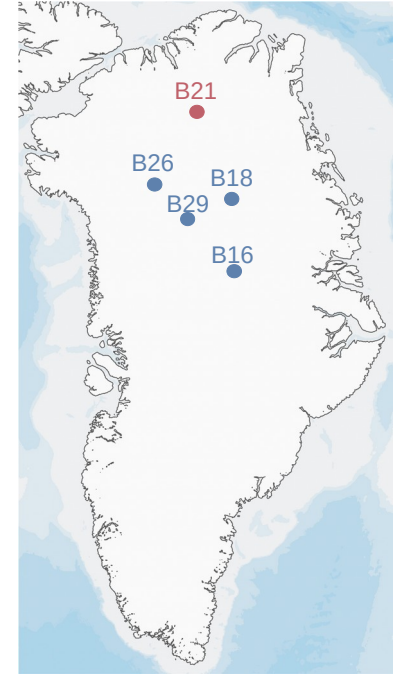
Arndt, J. E. et al. (2013). The International Bathymetric Chart of the Southern Ocean (IBSCO) Version 1.0 – A new bathymetric compilation covering circum-Antarctic waters. Geophysical Research Letters.

Examples - B21



— Herron & Langway (1980)

— Cell Model Approach



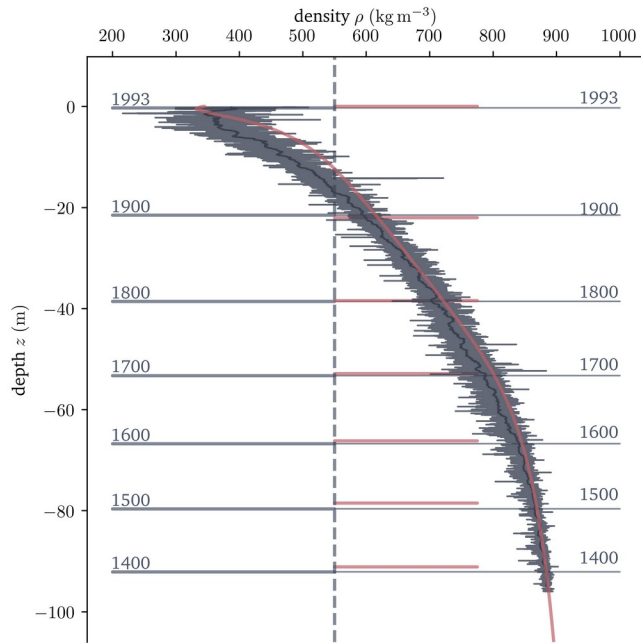
Wilhelms, F. (2000). Density of ice core ngt27C94.2 from the North Greenland Traverse. PANGAEA.

Miller, H. and Schwager, M. (2000). Accumulation rate and stable oxygen isotope ratios of ice core ngt27C94.2 from the North Greenland Traverse. PANGAEA.

Amante, C. and Eakins, B. W. (2009). ETOPO1 1 Arc-Minute Global Relief Model: Procedures, Data Source, and Analysis. NOAA.

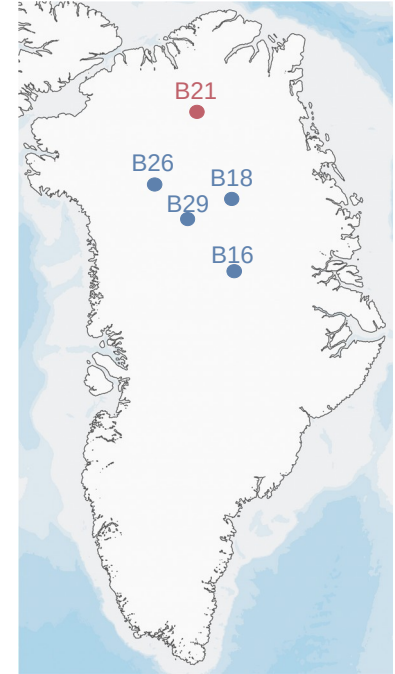
Arndt, J. E. et al. (2013). The International Bathymetric Chart of the Southern Ocean (IBSCO) Version 1.0 – A new bathymetric compilation covering circum-Antarctic waters. Geophysical Research Letters.

Examples - B21



— Herron & Langway (1980)

— Cell Model Approach



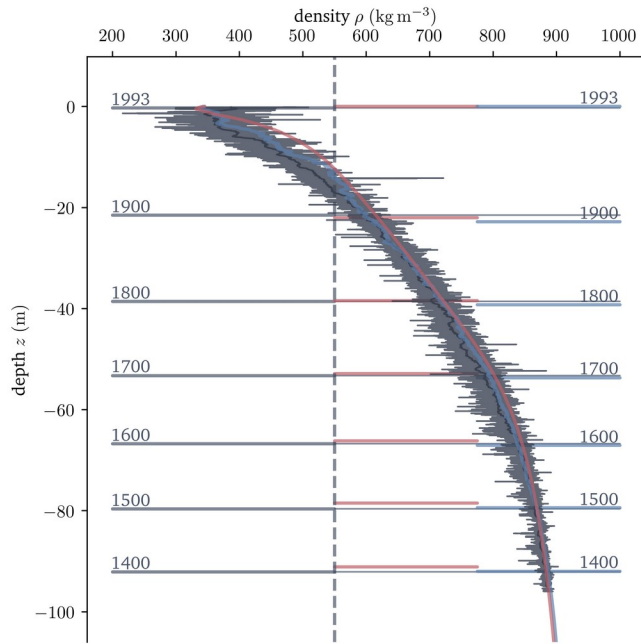
Wilhelms, F. (2000). Density of ice core ngt27C94.2 from the North Greenland Traverse. PANGAEA.

Miller, H. and Schwager, M. (2000). Accumulation rate and stable oxygen isotope ratios of ice core ngt27C94.2 from the North Greenland Traverse. PANGAEA.

Amante, C. and Eakins, B. W. (2009). ETOPO1 1 Arc-Minute Global Relief Model: Procedures, Data Source, and Analysis. NOAA.

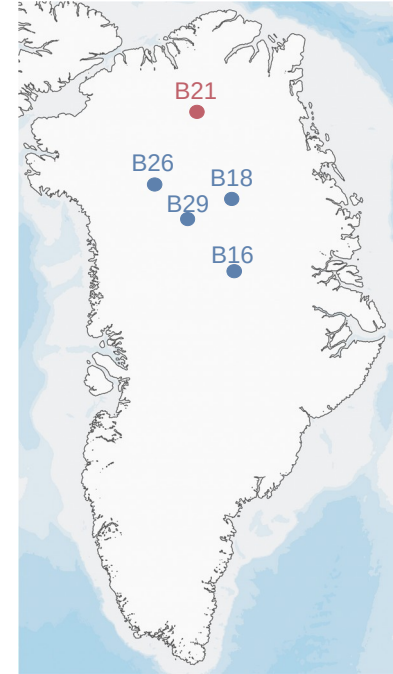
Arndt, J. E. et al. (2013). The International Bathymetric Chart of the Southern Ocean (IBSCO) Version 1.0 – A new bathymetric compilation covering circum-Antarctic waters. Geophysical Research Letters.

Examples - B21



— Herron & Langway (1980)

— Cell Model Approach



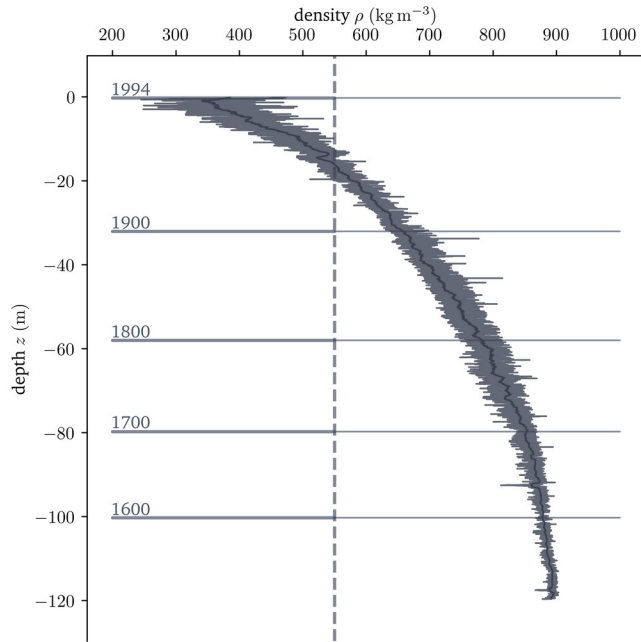
Wilhelms, F. (2000). Density of ice core ngt27C94.2 from the North Greenland Traverse. PANGAEA.

Miller, H. and Schwager, M. (2000). Accumulation rate and stable oxygen isotope ratios of ice core ngt27C94.2 from the North Greenland Traverse. PANGAEA.

Amante, C. and Eakins, B. W. (2009). ETOPO1 1 Arc-Minute Global Relief Model: Procedures, Data Source, and Analysis. NOAA.

Arndt, J. E. et al. (2013). The International Bathymetric Chart of the Southern Ocean (IBSCO) Version 1.0 – A new bathymetric compilation covering circum-Antarctic waters. Geophysical Research Letters.

Examples - B26

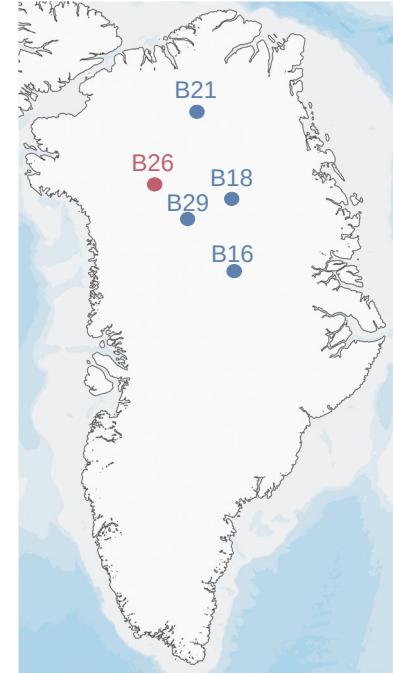


Miller, H. and Schwager, M. (2000). Density of ice core ngt37C95.2 from the North Greenland Traverse. PANGAEA.

Miller, H. and Schwager, M. (2000). Accumulation rate and stable oxygen isotope ratios of ice core ngt37C95.2 from the North Greenland Traverse. PANGAEA.

— Herron & Langway (1980)

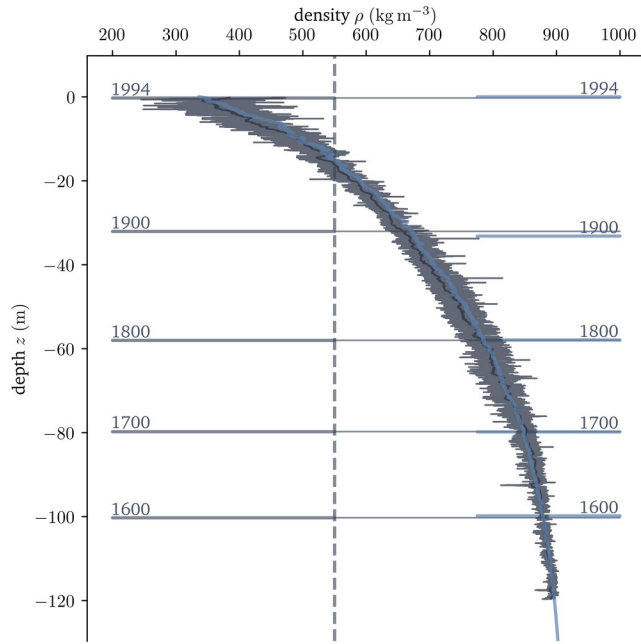
— Cell Model Approach



Amante, C. and Eakins, B. W. (2009). ETOPO1 1 Arc-Minute Global Relief Model: Procedures, Data Source, and Analysis. NOAA.

Arndt, J. E. et al. (2013). The International Bathymetric Chart of the Southern Ocean (IBSCO) Version 1.0 – A new bathymetric compilation covering circum-Antarctic waters. Geophysical Research Letters.

Examples - B26

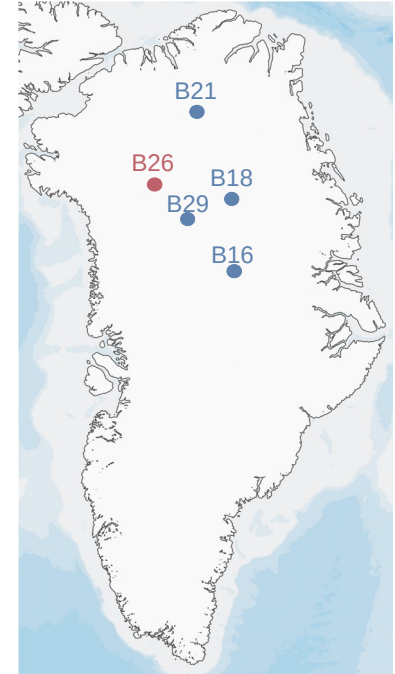


Miller, H. and Schwager, M. (2000). Density of ice core ngt37C95.2 from the North Greenland Traverse. PANGAEA.

Miller, H. and Schwager, M. (2000). Accumulation rate and stable oxygen isotope ratios of ice core ngt37C95.2 from the North Greenland Traverse. PANGAEA.

— Herron & Langway (1980)

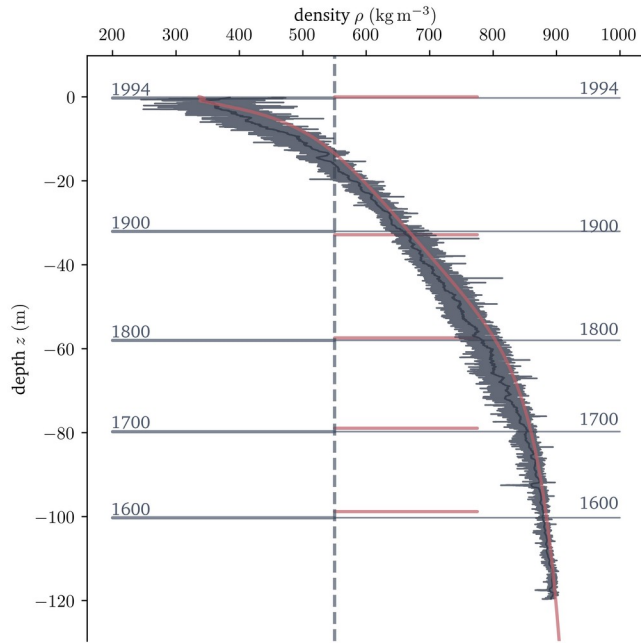
— Cell Model Approach



Amante, C. and Eakins, B. W. (2009). ETOPO1 1 Arc-Minute Global Relief Model: Procedures, Data Source, and Analysis. NOAA.

Arndt, J. E. et al. (2013). The International Bathymetric Chart of the Southern Ocean (IBSCO) Version 1.0 – A new bathymetric compilation covering circum-Antarctic waters. Geophysical Research Letters.

Examples - B26

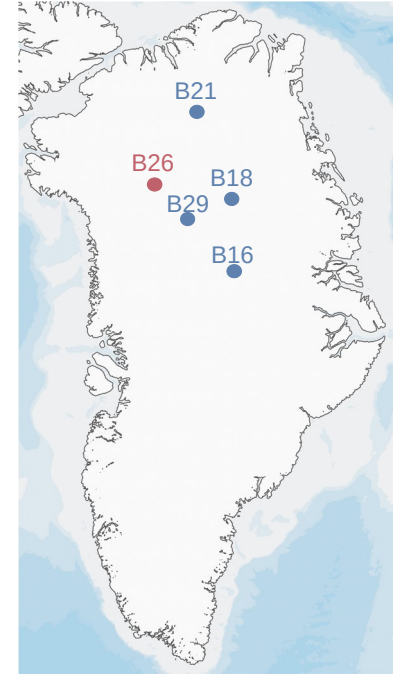


Miller, H. and Schwager, M. (2000). Density of ice core ngt37C95.2 from the North Greenland Traverse. PANGAEA.

Miller, H. and Schwager, M. (2000). Accumulation rate and stable oxygen isotope ratios of ice core ngt37C95.2 from the North Greenland Traverse. PANGAEA.

— Herron & Langway (1980)

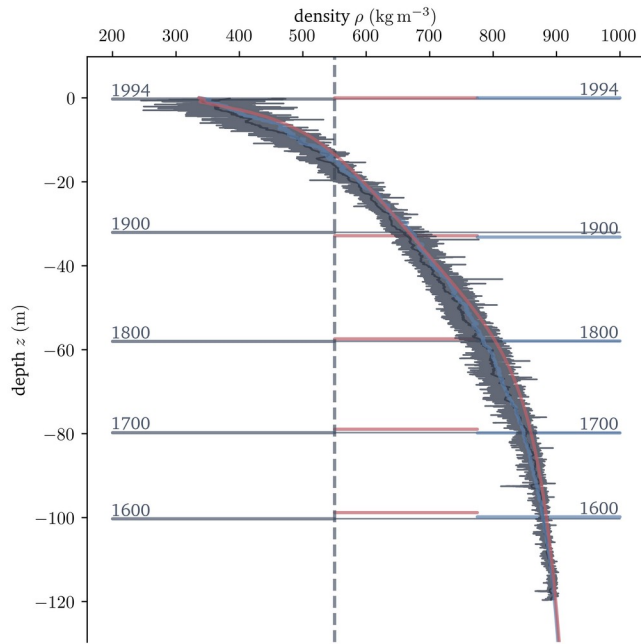
— Cell Model Approach



Amante, C. and Eakins, B. W. (2009). ETOPO1 1 Arc-Minute Global Relief Model: Procedures, Data Source, and Analysis. NOAA.

Arndt, J. E. et al. (2013). The International Bathymetric Chart of the Southern Ocean (IBSCO) Version 1.0 – A new bathymetric compilation covering circum-Antarctic waters. Geophysical Research Letters.

Examples - B26

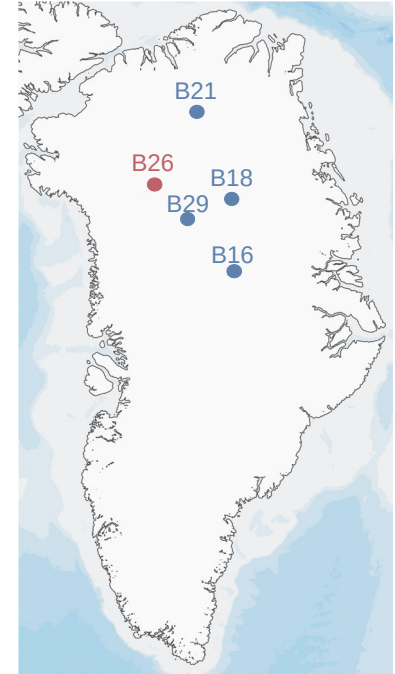


— Herron & Langway (1980)

— Cell Model Approach

Miller, H. and Schwager, M. (2000). Density of ice core ngt37C95.2 from the North Greenland Traverse. PANGAEA.

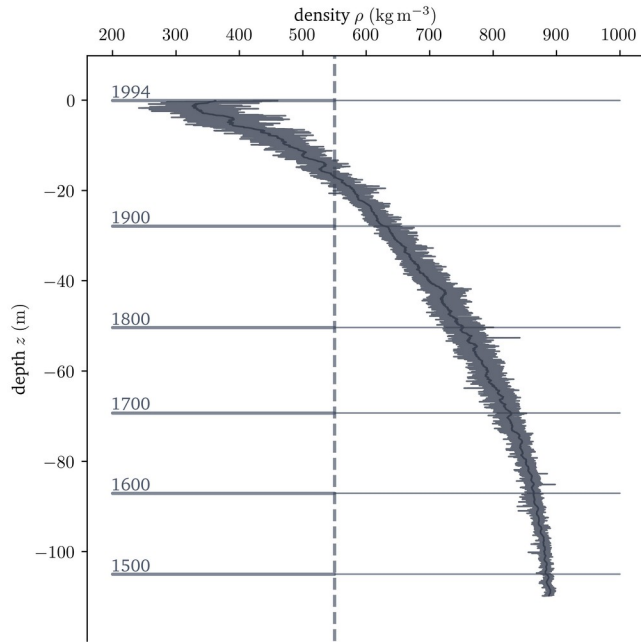
Miller, H. and Schwager, M. (2000). Accumulation rate and stable oxygen isotope ratios of ice core ngt37C95.2 from the North Greenland Traverse. PANGAEA.



Amante, C. and Eakins, B. W. (2009). ETOPO1 1 Arc-Minute Global Relief Model: Procedures, Data Source, and Analysis. NOAA.

Arndt, J. E. et al. (2013). The International Bathymetric Chart of the Southern Ocean (IBSCO) Version 1.0 – A new bathymetric compilation covering circum-Antarctic waters. Geophysical Research Letters.

Examples - B29

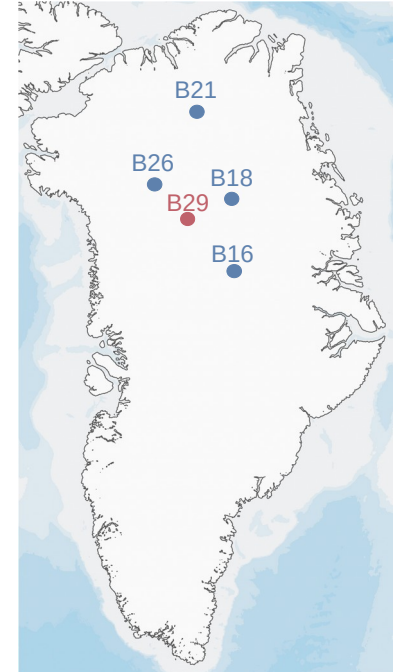


Miller, H. and Schwager, M. (2000). Density of ice core ngt42C95.2 from the North Greenland Traverse. PANGAEA.

Miller, H. and Schwager, M. (2000). Accumulation rate and stable oxygen isotope ratios of ice core ngt42C95.2 from the North Greenland Traverse. PANGAEA.

— Herron & Langway (1980)

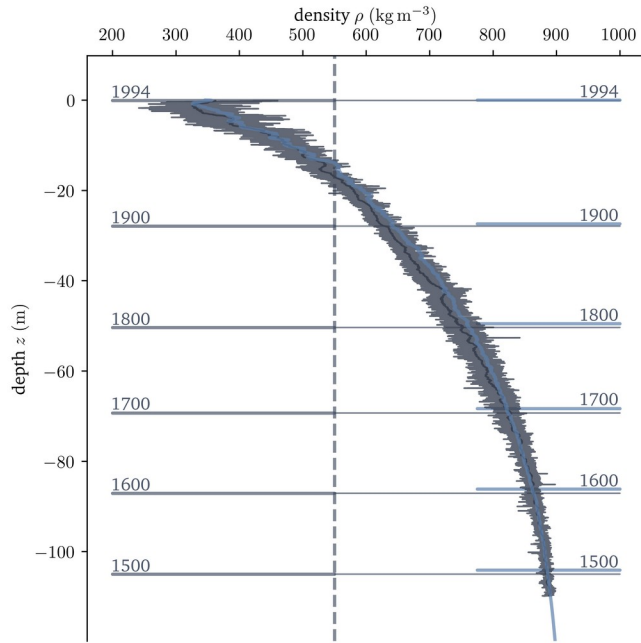
— Cell Model Approach



Amante, C. and Eakins, B. W. (2009). ETOPO1 1 Arc-Minute Global Relief Model: Procedures, Data Source, and Analysis. NOAA.

Arndt, J. E. et al. (2013). The International Bathymetric Chart of the Southern Ocean (IBSCO) Version 1.0 – A new bathymetric compilation covering circum-Antarctic waters. Geophysical Research Letters.

Examples - B29

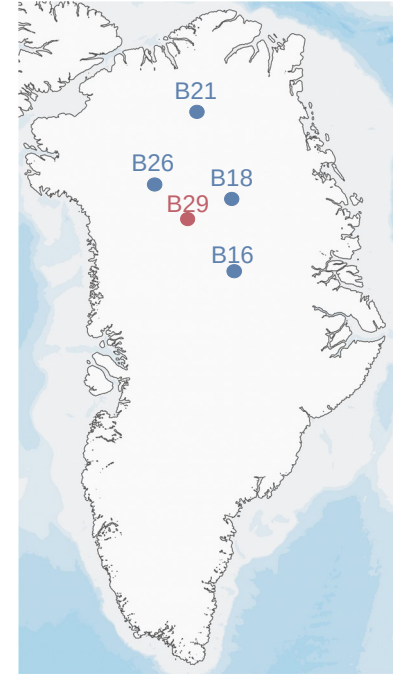


Miller, H. and Schwager, M. (2000). Density of ice core ngt42C95.2 from the North Greenland Traverse. PANGAEA.

Miller, H. and Schwager, M. (2000). Accumulation rate and stable oxygen isotope ratios of ice core ngt42C95.2 from the North Greenland Traverse. PANGAEA.

— Herron & Langway (1980)

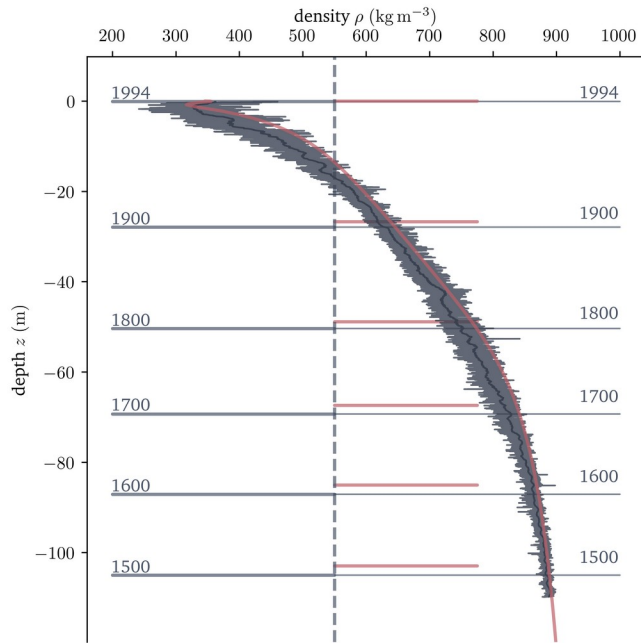
— Cell Model Approach



Amante, C. and Eakins, B. W. (2009). ETOPO1 1 Arc-Minute Global Relief Model: Procedures, Data Source, and Analysis. NOAA.

Arndt, J. E. et al. (2013). The International Bathymetric Chart of the Southern Ocean (IBSCO) Version 1.0 – A new bathymetric compilation covering circum-Antarctic waters. Geophysical Research Letters.

Examples - B29

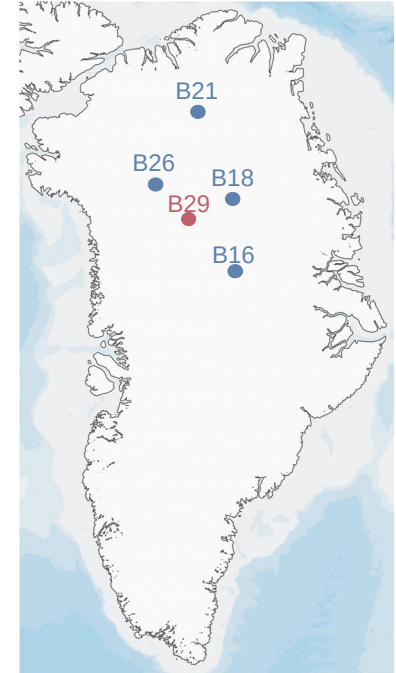


— Herron & Langway (1980)

— Cell Model Approach

Miller, H. and Schwager, M. (2000). Density of ice core ngt42C95.2 from the North Greenland Traverse. PANGAEA.

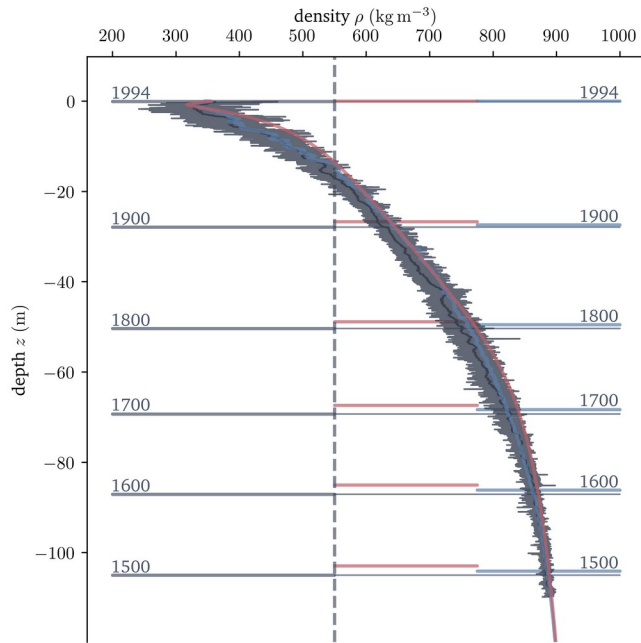
Miller, H. and Schwager, M. (2000). Accumulation rate and stable oxygen isotope ratios of ice core ngt42C95.2 from the North Greenland Traverse. PANGAEA.



Amante, C. and Eakins, B. W. (2009). ETOPO1 1 Arc-Minute Global Relief Model: Procedures, Data Source, and Analysis. NOAA.

Arndt, J. E. et al. (2013). The International Bathymetric Chart of the Southern Ocean (IBSCO) Version 1.0 – A new bathymetric compilation covering circum-Antarctic waters. Geophysical Research Letters.

Examples - B29

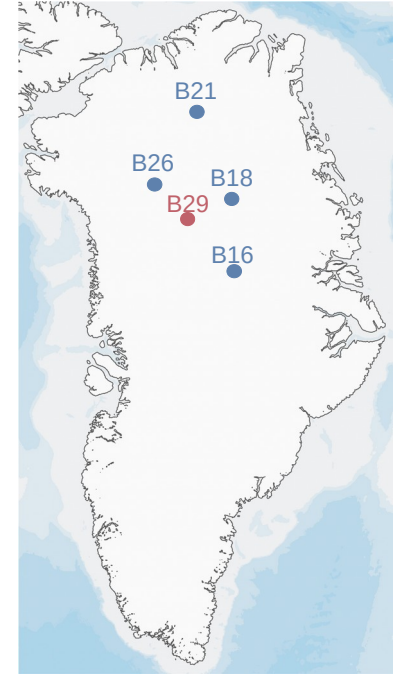


— Herron & Langway (1980)

— Cell Model Approach

Miller, H. and Schwager, M. (2000). Density of ice core ngt42C95.2 from the North Greenland Traverse. PANGAEA.

Miller, H. and Schwager, M. (2000). Accumulation rate and stable oxygen isotope ratios of ice core ngt42C95.2 from the North Greenland Traverse. PANGAEA.



Amante, C. and Eakins, B. W. (2009). ETOPO1 1 Arc-Minute Global Relief Model: Procedures, Data Source, and Analysis. NOAA.

Arndt, J. E. et al. (2013). The International Bathymetric Chart of the Southern Ocean (IBSCO) Version 1.0 – A new bathymetric compilation covering circum-Antarctic waters. Geophysical Research Letters.